RAIO-0818-61621

August 29, 2018

Docket No. 52-048

U.S. Nuclear Regulatory Commission
ATTN: Document Control Desk
One White Flint North
11555 Rockville Pike
Rockville, MD 20852-2738

SUBJECT: NuScale Power, LLC Response to NRC Request for Additional Information No. 164 (eRAI No. 8935) on the NuScale Design Certification Application

REFERENCES:
1. U.S. Nuclear Regulatory Commission, "Request for Additional Information No. 164 (eRAI No. 8935)," dated August 11, 2017
2. NuScale Power, LLC Response to NRC "Request for Additional Information No. 164 (eRAI 8935)'" dated October 6, 2017

The purpose of this letter is to provide the NuScale Power, LLC (NuScale) response to the referenced NRC Request for Additional Information (RAI).

The Enclosure to this letter contains NuScale's response to the following RAI Question from NRC eRAI No. 8935:

- 03.07.02-23

The response to RAI Question 03.07.02-24 was previously provided in Reference 2. The response to question 03.07.02-25 will be provided by December 20, 2019 and the response to question 03.07.02-26 will be provided by November 29, 2018.

This letter and the enclosed response make no new regulatory commitments and no revisions to any existing regulatory commitments.

If you have any questions on this response, please contact Marty Bryan at 541-452-7172 or at mbryan@nuscalepower.com.

Sincerely,

Jennie Wike
Manager, Licensing
NuScale Power, LLC

Distribution: Gregory Cranston, NRC, OWFN-8G9A
Samuel Lee, NRC, OWFN-8G9A
Marieliz Vera, NRC, OWFN-8G9A

Enclosure 1: NuScale Response to NRC Request for Additional Information eRAI No. 8935

Enclosure 1:

NuScale Response to NRC Request for Additional Information eRAI No. 8935

NuScale Power, LLC
1100 NE Circle Blvd., Suite 200 Corvalis, Oregon 97330, Office: 541.360.0500, Fax: 541.207.3928
www.nuscalepower.com

Response to Request for Additional Information
Docket No. 52-048

eRAI No.: 8935
Date of RAI Issue: 08/11/2017

NRC Question No.: 03.07.02-23

10 CFR 50 Appendix S requires that the safety functions of structures, systems, and components (SSCs) must be assured during and after the vibratory ground motion associated with the Safe Shutdown Earthquake (SSE) through design, testing, or qualification methods.

DSRS Section 3.7.2 provides guidance that, for soil-structure interaction (SSI) analysis for deeply embedded structures, proper consideration should be given to uncertainties associated with kinematic interaction, non-vertically propagating shear waves, sidewall impedance calculation, and other effects such as the development of gaps between the soil and structure specifically for strong-motion earthquakes. For non-vertically propagating shear waves, a sensitivity evaluation can be performed to determine whether this is an important effect to be included in the SSI analysis. Staff has not been able to identify how the applicant has considered these uncertainties associated with SSI of deeply embedded structures in the seismic analysis of NuScale Category I SSCs. Provide an explanation for what analyses the applicant has performed and how these uncertainties have been considered.

NuScale Response:

1.0 Background

1.1 DCA Soil Profiles

For the NuScale Design Certification Application (DCA), the soil structure interaction (SSI) analysis of the reactor building (RXB) was performed with four different soil profiles. The soil profiles are designated as Soil Type 11 (soft soil), Soil Type 8 (firm soil/soft rock), Soil Type 7 (rock), and Soil Type 9 (hard rock). The shear wave velocity profiles of these three soil profiles are shown in Figure 1-1.

The SSI analyses documented in the DCA were performed with vertically propagating seismic waves. This is a reasonable method, because, for non-uniform and soft soil profiles, the angle of incidence decreases as the wave propagates toward the surface, due to Snell's law.

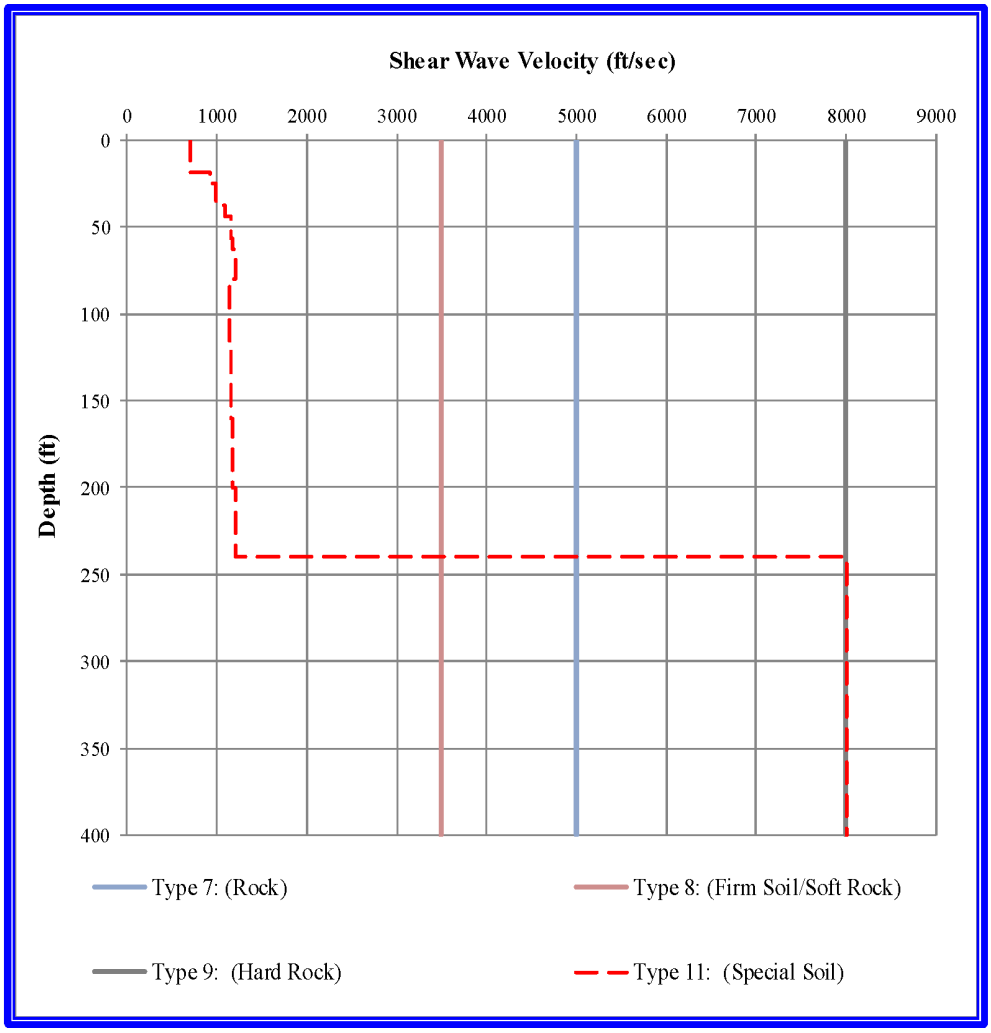

Figure 1-1. Low-Strain Shear Wave Velocity Profiles for Soil Types 7, 8, 9, and 11.

1.2 Definition of NuScale CSDRS

The horizontal and vertical certified seismic design response spectra (CSDRS) used for the evaluation of the NuScale RXB are shown in Figure 1-2. The horizontal CSDRS has a zero period acceleration (ZPA) of 0.5 g. The vertical CSDRS has a ZPA of 0.4 g.

It is important to note that:

- The CSDRS is the basis for the design of the RXB.
- The CSDRS is defined as the rock outcrop input at a foundation depth of 86′.
- The CSDRS is independent of the angle of incidence of the seismic waves.

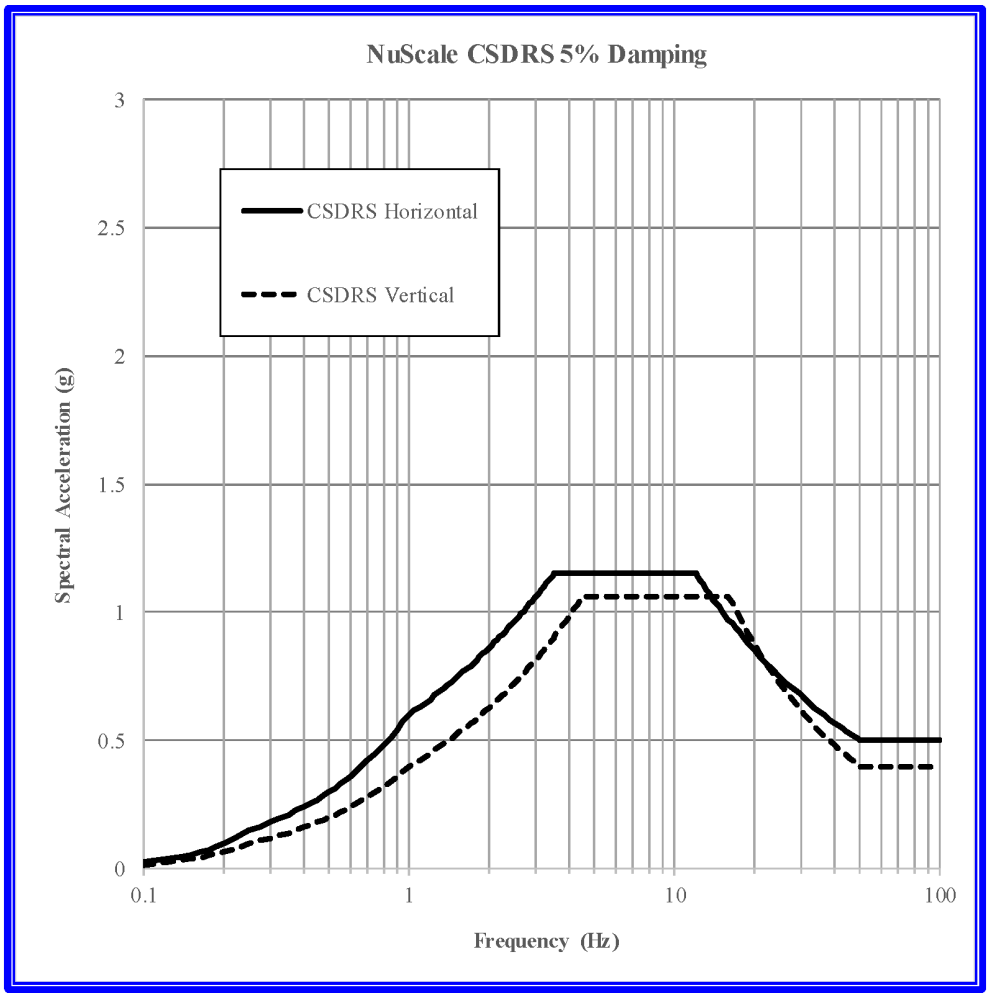

Figure 1-2. NuScale Horizontal and Vertical CSDRS.

2.0 SELECTION OF SOIL PROFILE

For this study, Soil Type 7 was selected. As shown in Figure 1-1, this soil profile is uniform, and, thus, the effect of non-vertically propagating waves will be the most pronounced for this case.

3.0 RESPONSE OF FREE-FIELD TO NON-VERTICALLY PROPAGATING WAVES

This section presents the response of the free-field to non-vertically propagating waves. Analysis results will show the effect of non-vertically propagating waves on the CSDRS.

As discussed in Section 2.0, the properties of Soil Type 7 were used.

3.1 Analysis Approach

To determine the response of the free-field to vertically or non-vertically propagating waves, a SASSI2010 model consisting only of the free-field soil, without any structure, was analyzed.

The coordinate system and variables used to define the wave propagation throughout this document are shown in Figure 3-1.

Note that vertically propagating SV and SH waves produce only horizontal ground motion, while vertically propagating P waves produce only vertical ground motion. Non-vertically propagating SV and P waves produce both horizontal and vertical ground motion, while non-vertically propagating SH waves still produce only horizontal ground motion.

For this study, angles of incidence of wave propagation, α, equal to 0°, 17°, and 30° are used. The angle of incidence is measured from the vertical axis and in the X-Z plane, as shown in Figure 3-1. Thus, $\alpha = 0°$ corresponds to a vertically propagating wave with an apparent wave velocity of infinity. Since Soil Type 7 is nearly a uniform soil profile with a shear wave velocity, Vs, of 5,000 ft/sec, $\alpha = 17°$ corresponds to an apparent wave velocity of approximately Vs/sin(17°) = 17,100 ft/sec (5.2 km/sec) and $\alpha = 30°$ corresponds to an apparent wave velocity of approximately Vs/sin(30°) = 10,000 ft/sec (3.0 km/sec).

Since the CSDRS is defined as the rock outcrop motion at the foundation level, a site response analysis must be performed first to obtain the in-layer motions to be input to SASSI2010.

3.1.1 Site Response Analysis

The SHAKE2000 program was used to perform the site response analysis for Soil Type 7 to calculate the average strain-compatible soil properties provided in FSAR Table 3.7.1-15. In the site response analyses, the CSDRS-compatible time histories are input as rock outcrop motions at the elevation of the RXB foundation bottom. The SHAKE2000 program provides the motions at the soil surface (grade level) and the in-layer motions at the bottom of the RXB foundation to be input to SASSI2010.

For vertically propagating wave cases, either the motions at the surface or the in-layer motions at the bottom of the RXB foundation can be used as input to SASSI and the corresponding SASSI results will be identical. For non-vertically propagating wave cases, the motion at the top surface, or grade level, must be used as input to SASSI2010.

3.1.2 SASSI Analysis with Free-Field

The surface motions obtained from the SHAKE2000 site response analysis in the previous section are applied to a SASSI model of the free-field, without any structure. The control point is

specified to be at the surface. The angle of incidence is defined at the half-space location, which is at a depth of 300′ in this case. See Figure 5-1 for a sketch of the input.

Note that in SASSI2010, the location of the control point and angle of incidence are defined in the SITE module, where the properties of all the soil layers and the location of the halfspace are defined. Mode shapes are calculated based on all soil layers. The mode shapes define the ground motions (vertically propagating and non-vertically propagating) at each soil layer. The control point defines the elevation where the modes shapes are normalized. In this way, by defining the in-layer motion at the control point elevation, SASSI automatically generates the motion at all of the other layers.

For the non-vertically propagating wave cases, the control point must be at the surface. If the control point is at the foundation level, there is a shift in the soil column frequency of non-vertically propagating waves. However, since the in-layer motion at the foundation level is determined for $\alpha = 0°$ in the site response analysis, there is a mismatch in the soil column frequency between the in-layer motion and the non-vertically propagating wave. This results in incorrect responses being generated.

For this reason, the time history responses at the ground surface corresponding to the CSDRS input at the foundation level obtained from vertically propagating waves are used as input motions, with the control point defined at the ground surface for all three angles of incidence for this study.

The resultant in-column response motions at the surface are compared in Section 3.2.1.

The resultant in-column response motions at the foundation level are compared in Section 3.2.2.

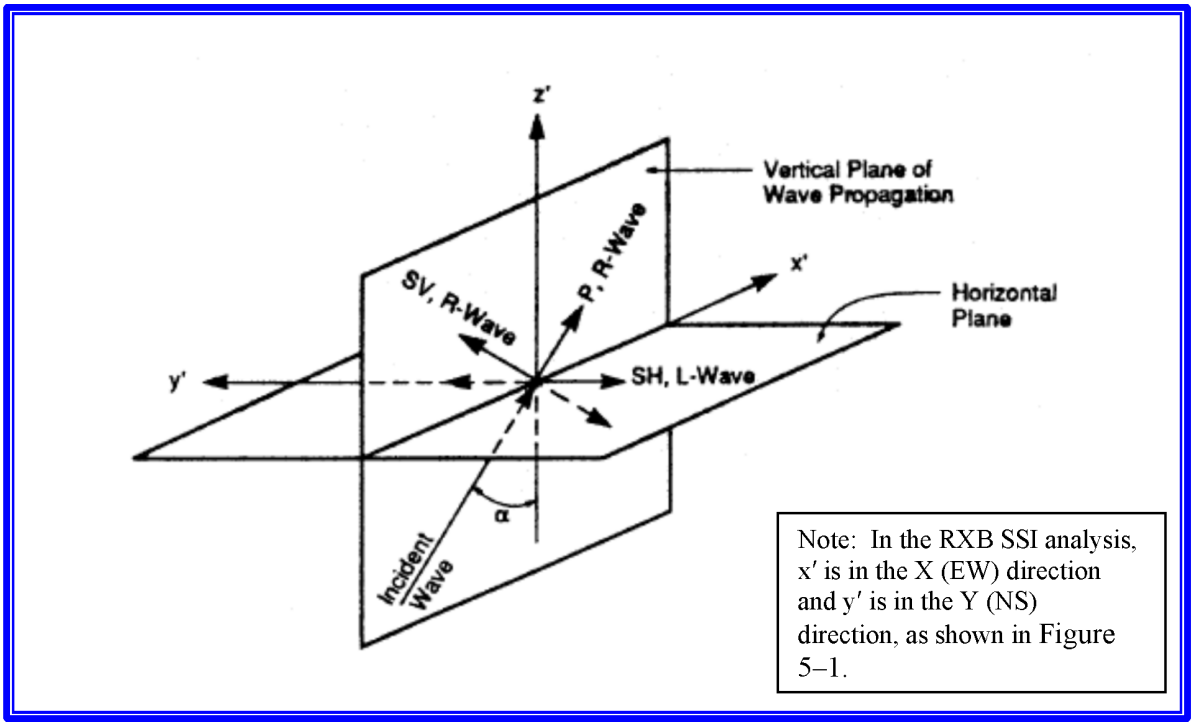

Figure 3-1. Definition of Angle of Incidence, α (from SASSI2010 manual).

3.2 Comparison of Free-Field Motion at FIRS Horizon with Design Basis Case

This section presents comparisons of ARS at the ground surface (Node 1) and at a depth of 85′ (Node 15) for the free-field-only case. There is no SSI effect in the free-field case.

Comparisons of X-response ARS at the surface due to SV and P-waves are presented in Section 3.2.1.

Comparisons of X-response ARS at a depth of 85′ due to SV and P-waves are presented in Section 3.2.2.

Comparisons of Z-response ARS at the surface due to SV and P-waves are presented in Section 3.2.3.

Comparisons of Z-response ARS at a depth of 85′ due to SV and P-waves are presented in Section 3.2.4.

Note that in the legends of the figures, “X/SV” means the X-response due to SV-wave input; “X/P” means the X-response due to P-wave input; etc. Also, when a response is referred to as “CSDRS”, it means the “response due to the CSDRS-compatible input time history.”

As can be seen from Figure 3-1, the SH-waves do not have any coupling responses; therefore, the horizontal, in-layer motion in the soil column from inclined waves is nearly identical to the horizontal, in-layer motion from vertical waves. For this reason, results from non-vertically propagating SH-waves will not be presented. (The term in-layer motion refers to the ground motion which includes the effect of the soil above, that is, not an outcrop motion.)

3.2.1 Free-Field X-Response ARS at Surface Due to SV- and P-Waves

Figure 3-2 shows the X-response ARS at the surface due to SV-waves for α = 0°, 17°, and 30°. Note that these curves are identical, because the control point is at the ground surface. The CSDRS at the rock outcrop (dashed line) is shown for reference only. All three ARS at the surface due to SV-waves for α = 0°, 17°, and 30° are identical.

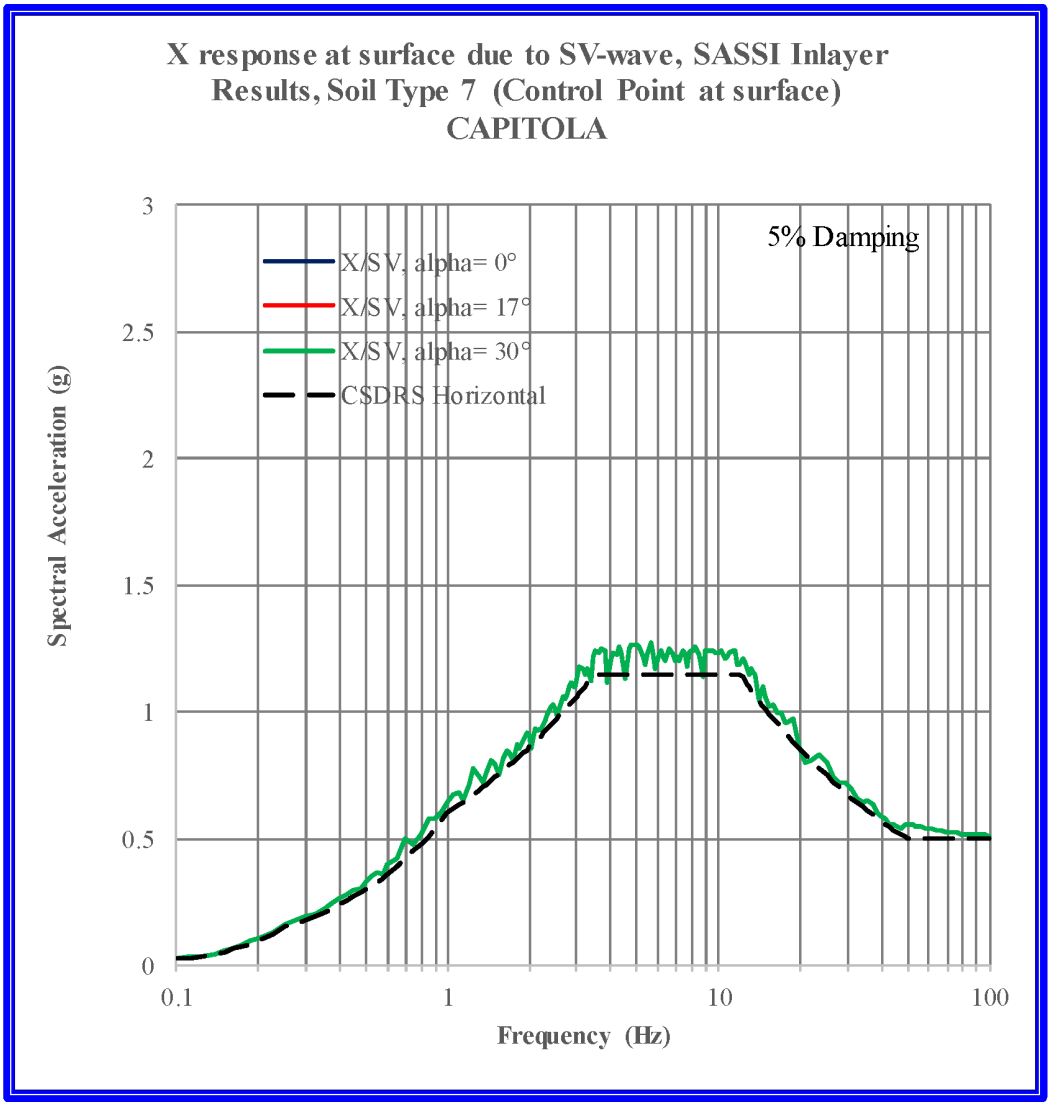

Figure 3-2. Soil Type 7 - Free-Field Uncoupled East-West (X) ARS at Surface, Capitola Input.

Figure 3-3 shows the X-response ARS at the ground surface due to SV and P-waves for α = 17°. The combined response obtained by SRSS combination of the two curves is also shown. Note that since the control point is at the ground surface, the X/SV curves for α = 0° and α = 17° are identical.

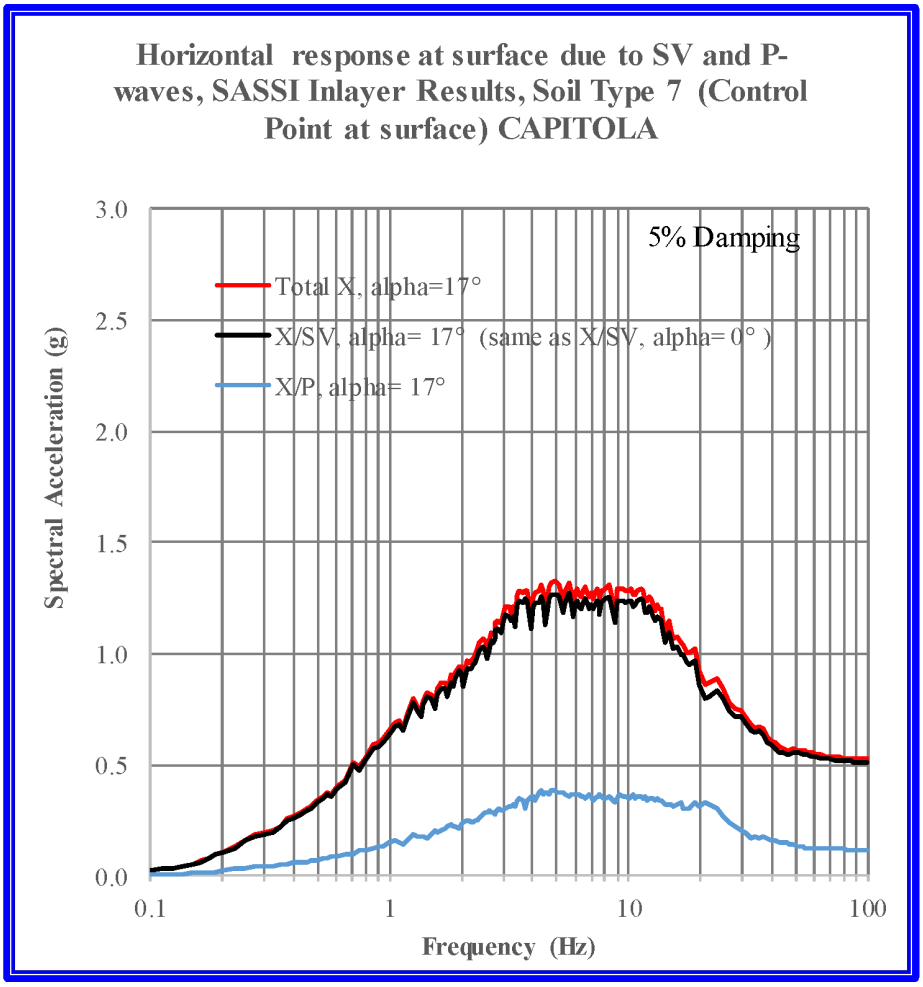

Figure 3-3. Soil Type 7 - Free-Field East-West (X) ARS at Surface, Capitola Input, α = 17°.

Figure 3-4 shows the X-response ARS at the ground surface due to SV and P-waves for α = 30°. The combined response obtained by SRSS combination of the two curves is also shown. Note that since the control point is at the ground surface, the X/SV curves for α = 0° (CSDRS) and α = 17° are identical and, thus, the total X curve will be higher than the CSDRS curve.

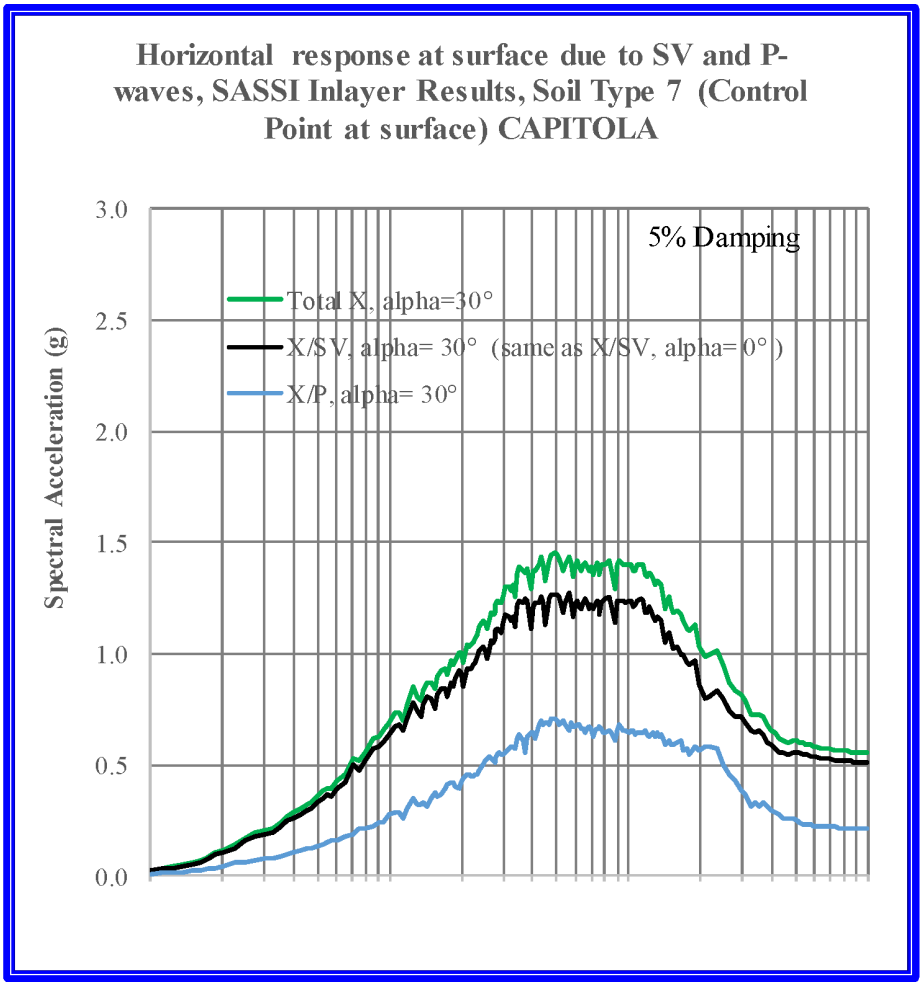

Figure 3-4. Soil Type 7 - Free-Field East-West (X) ARS at Surface, Capitola Input, alpha = 30°.

Figure 3-5 shows a comparison of the combined X-response ARS at the ground surface for α = 0°, 17°, and 30°. Note that the α = 0° curve represents the CSDRS motion at this depth. The α = 17° and α = 30° curves include the horizontal response due to P-waves and, thus, exceed the CSDRS that was chosen as the design basis.

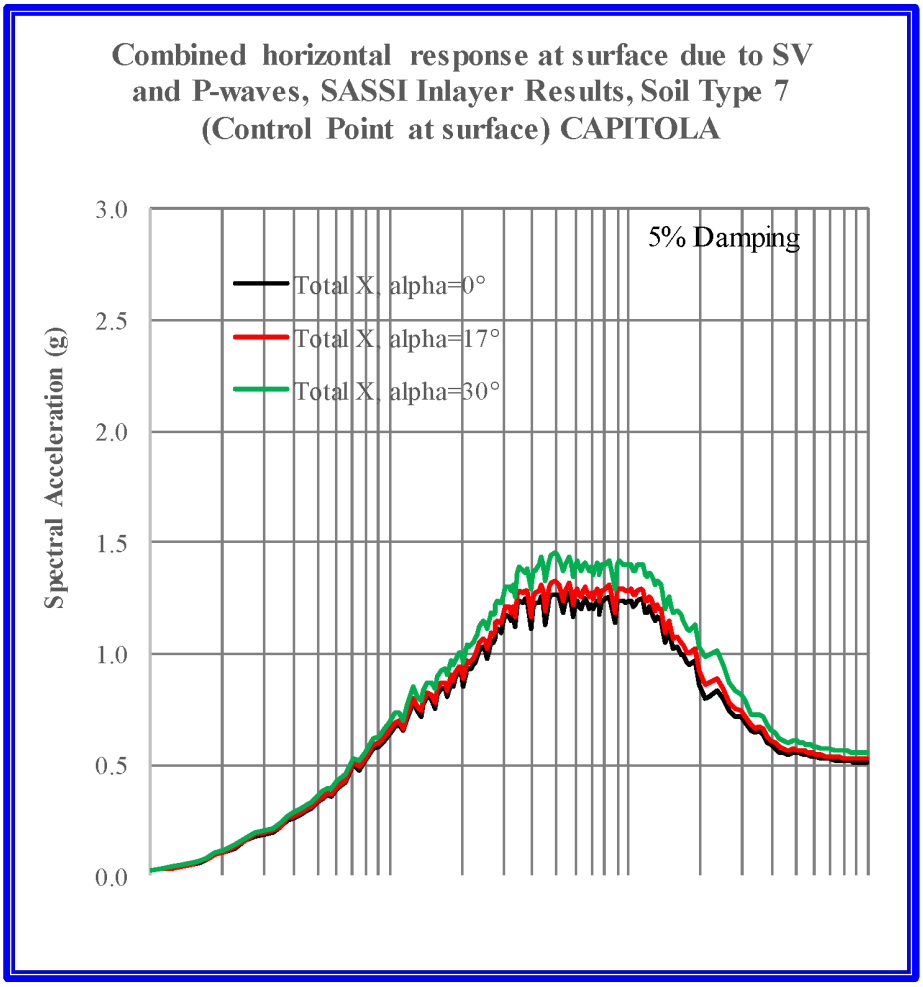

Figure 3-5. Soil Type 7 - Comparison of Combined Free-Field East-West (X) ARS at Surface, Capitola Input.

3.2.2 Free-Field X-Response ARS at Depth 85′ Due to SV and P-Waves

Figure 3-6 shows the X-response ARS at a depth of 85′ due to SV-waves for α = 0°, 17°, and 30°. Note that the α = 0° curve represents the CSDRS motion (or FIRS) at this depth. The CSDRS at the rock outcrop (dashed line) is shown for reference only. The CSDRS is exceeded by the X/SV ARS.

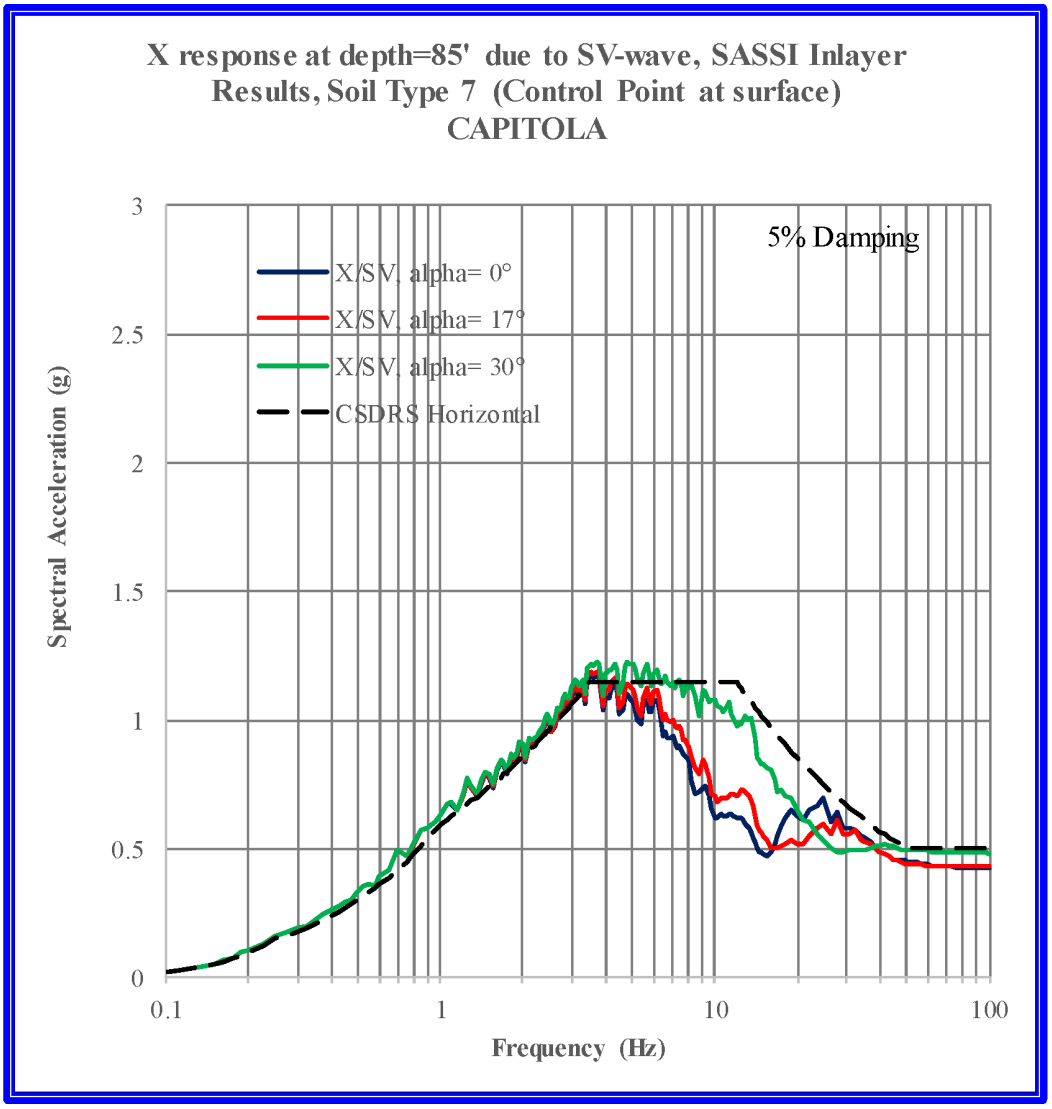

Figure 3-6. Soil Type 7 - Free-Field Uncoupled East-West (X) ARS at Depth 85′, Capitola Input.

Figure 3-7 shows the X-response ARS at a depth of 85′ due to SV and P-waves for α = 17°. The combined response obtained by SRSS combination of the two curves is also shown. Also shown is the α = 0° response (solid black curve), which represents the CSDRS motion (or FIRS) at this depth. The CSDRS is exceeded by the total X and X/SV ARS.

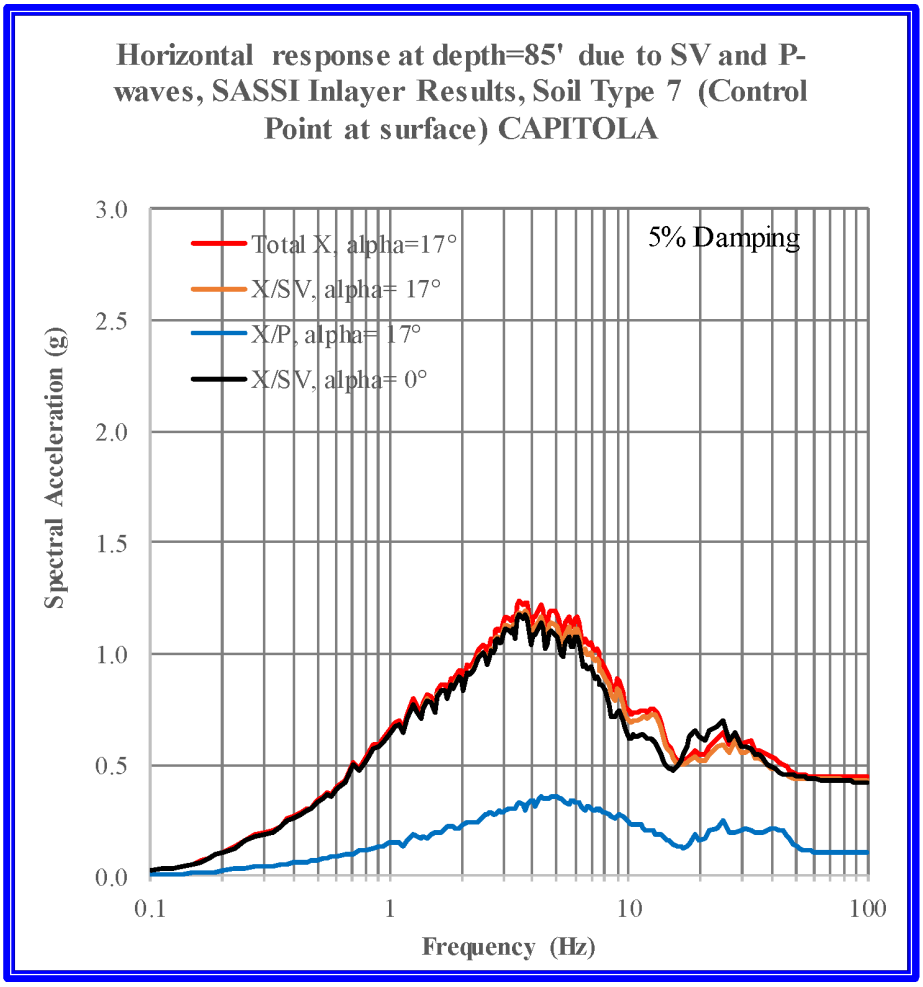

Figure 3-7. Soil Type 7 - Free-Field East-West (X) ARS at Depth 85′, Capitola Input, alpha = 17°.

Figure 3-8 shows the X-response ARS at a depth of 85′ due to SV and P-waves for α = 30°. The combined response obtained by SRSS combination of the two curves is also shown. Also shown is the α = 0° response (solid black curve), which represents the CSDRS motion (or FIRS) at this depth. The CSDRS is exceeded by the total X and X/SV ARS.

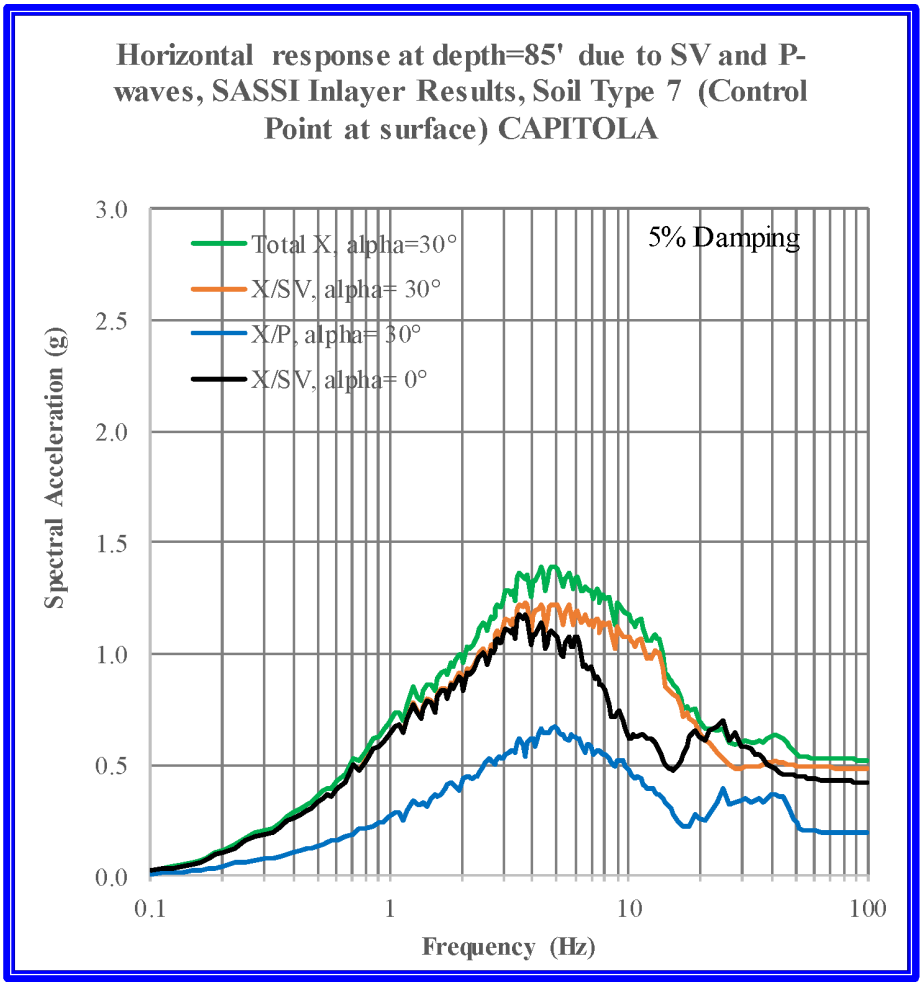

Figure 3-8. Soil Type 7 - Free-Field East-West (X) ARS at Depth 85′, Capitola Input, alpha = 30°.

Figure 3-9 shows a comparison of the combined X-response ARS at a depth of 85′ for α = 0°, 17°, and 30°. Note that the α = 0° curve represents the CSDRS motion (or FIRS) at this depth. The α = 17° and α = 30° curves include the coupling term (horizontal response due to P-wave) and, thus, exceed the CSDRS that was chosen as the design basis. The motion for the α = 30° case becomes conservative when the coupling term is included.

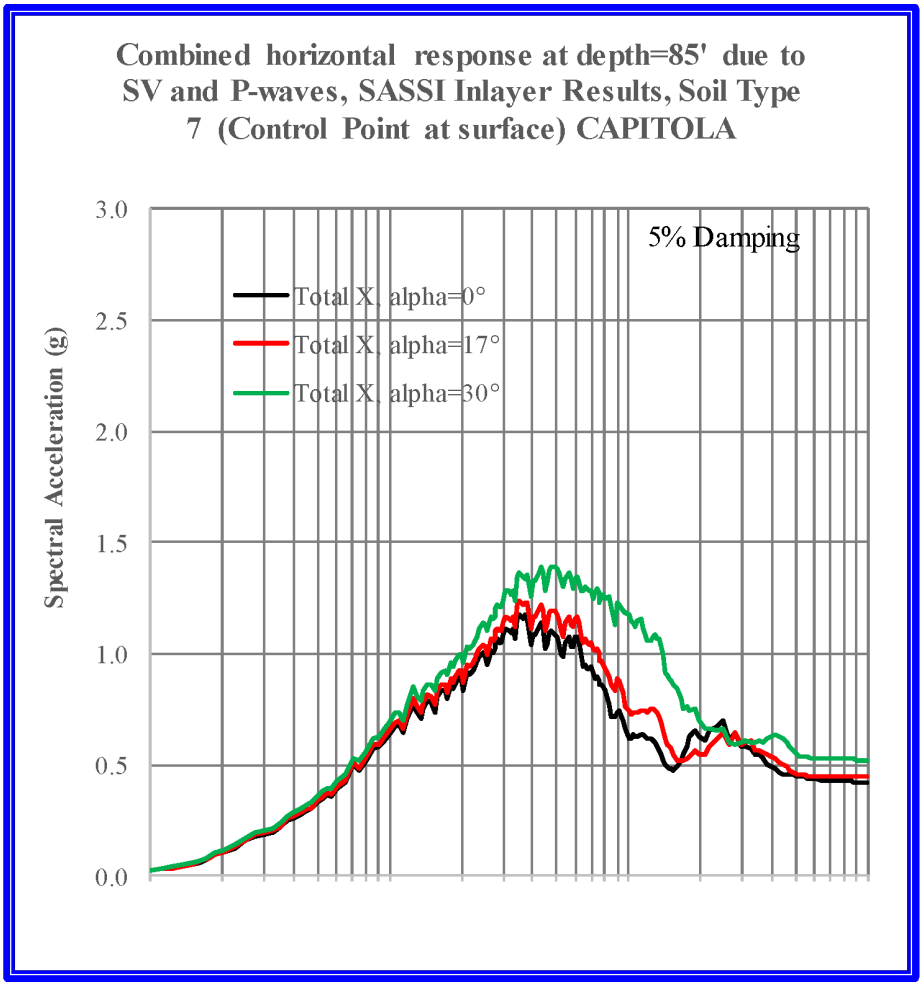

Figure 3-9. Soil Type 7 - Comparison of Combined Free-Field East-West (X) ARS at Depth 85′, Capitola Input, alpha = 0°, 17°, 30°.

3.2.3 Free-Field Z-Response ARS at Surface Due to SV and P-Waves

Figure 3-10 shows the Z-response ARS at the surface due to P-waves for α = 0°, 17°, and 30°. Note that these curves are identical because the control point is at the ground surface. The CSDRS at the rock outcrop (dashed line) is shown for reference only.

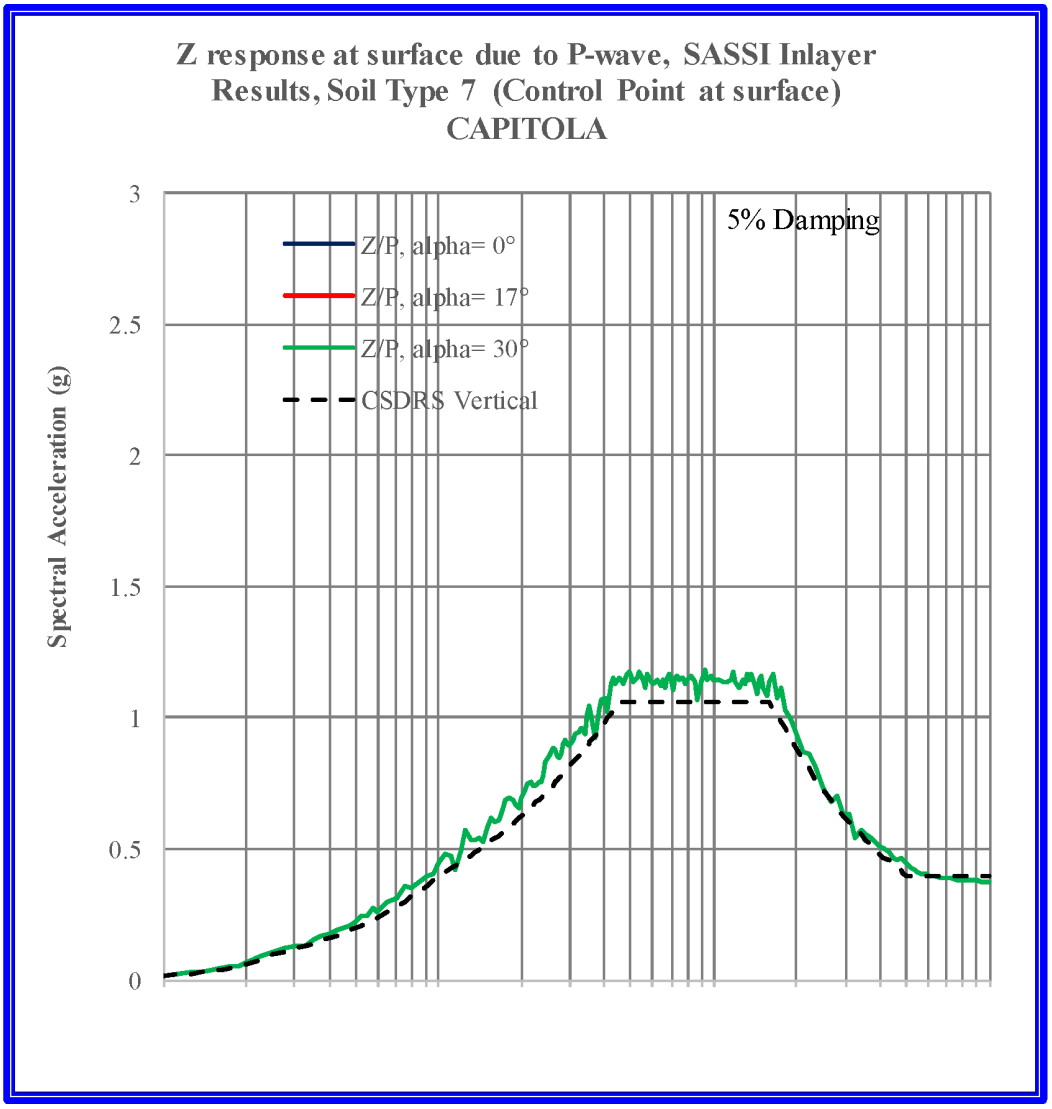

Figure 3-10. Soil Type 7 - Free-Field Uncoupled Vertical (Z) ARS at Surface, Capitola Input, alpha = 0°, 17°, 30°.

Figure 3-11 shows the Z-response ARS at the ground surface due to SV and P-waves for α = 17°. The combined response obtained by SRSS combination of the two curves is also shown. Note that since the control point is at the ground surface, the Z/P curves for α = 0° and α = 17° are identical. The CSDRS is exceeded by the total Z ARS.

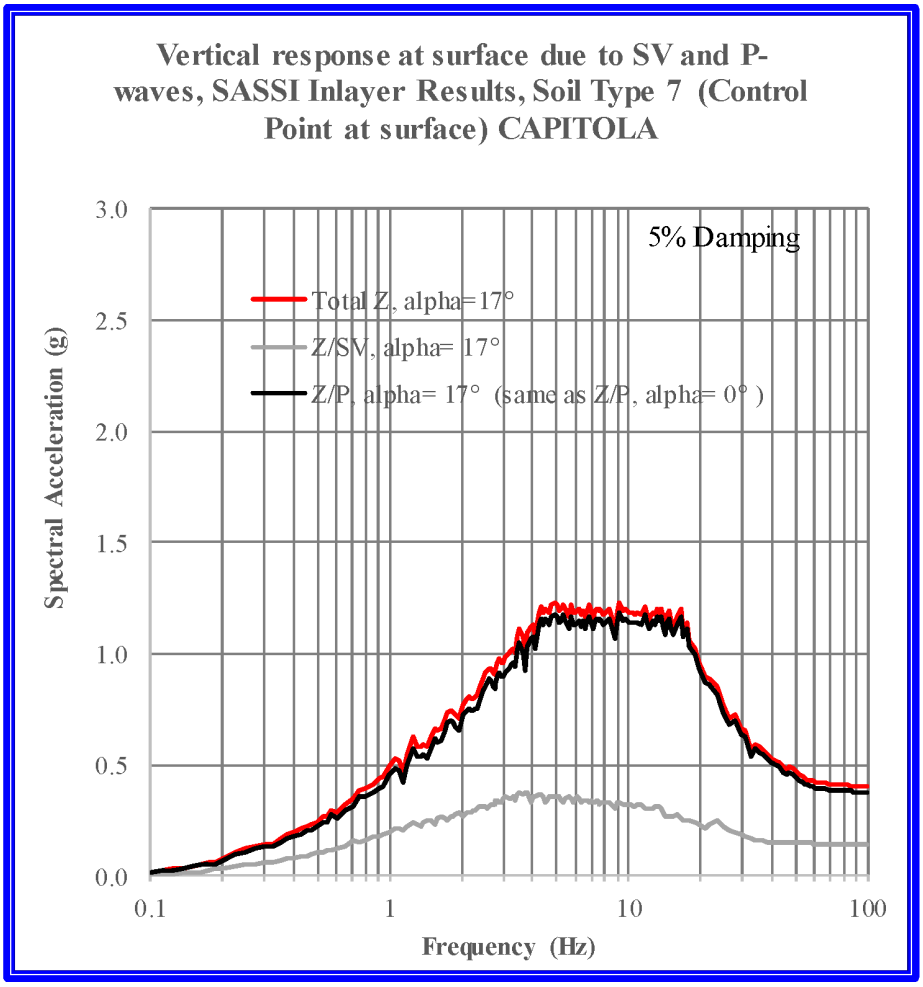

Figure 3-11. Soil Type 7 - Free-Field Vertical (Z) ARS at Surface, Capitola Input, alpha = 17°.

Figure 3-12 shows the Z-response ARS at the ground surface due to SV and P-waves for α = 30°. The combined response obtained by SRSS combination of the two curves is also shown. Note that since the control point is at the ground surface, the Z/P curves for α = 0° and α = 30° are identical. The CSDRS is exceeded by the total Z ARS.

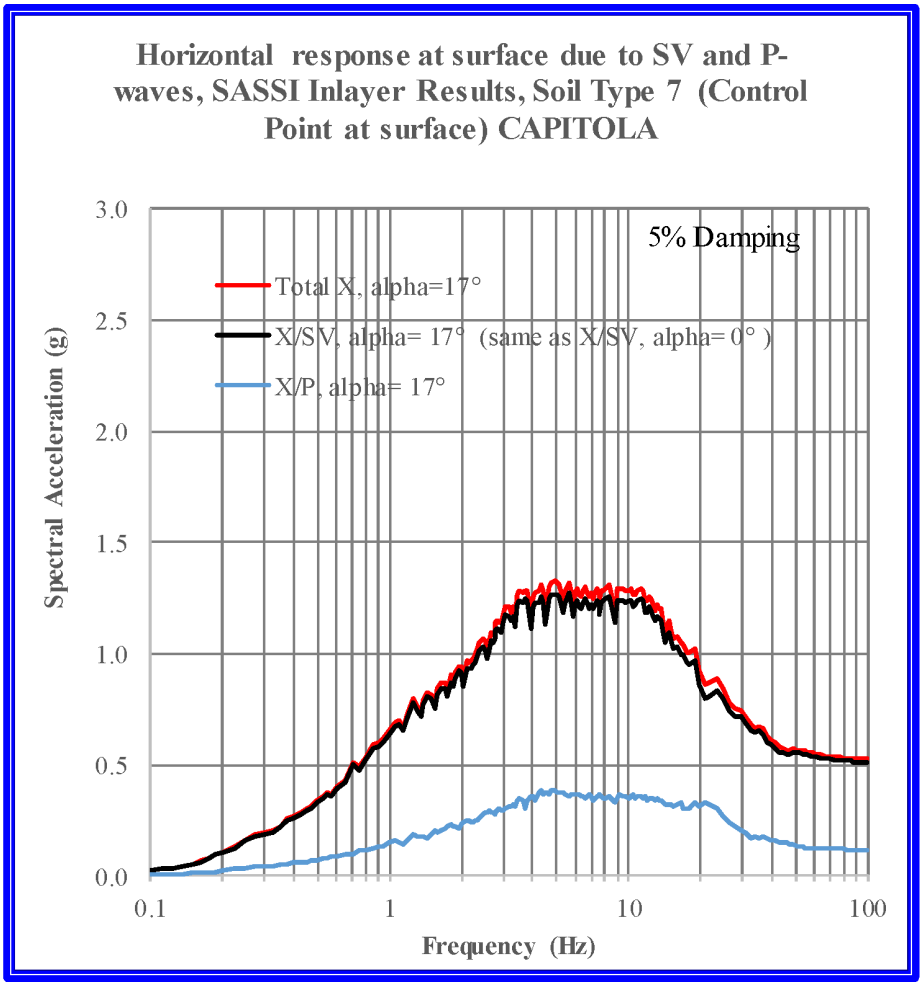

Figure 3-12. Soil Type 7 - Free-Field Vertical (Z) ARS at Surface, Capitola Input, alpha = 30°.

Figure 3-13 shows a comparison of the combined Z-response ARS at the ground surface for α = 0°, 17°, and 30°. Note that the α = 0° curve represents the CSDRS motion at this depth. The α = 17° and α = 30° curves include the vertical response due to SV-waves and thus exceed the CSDRS that was chosen as the design basis.

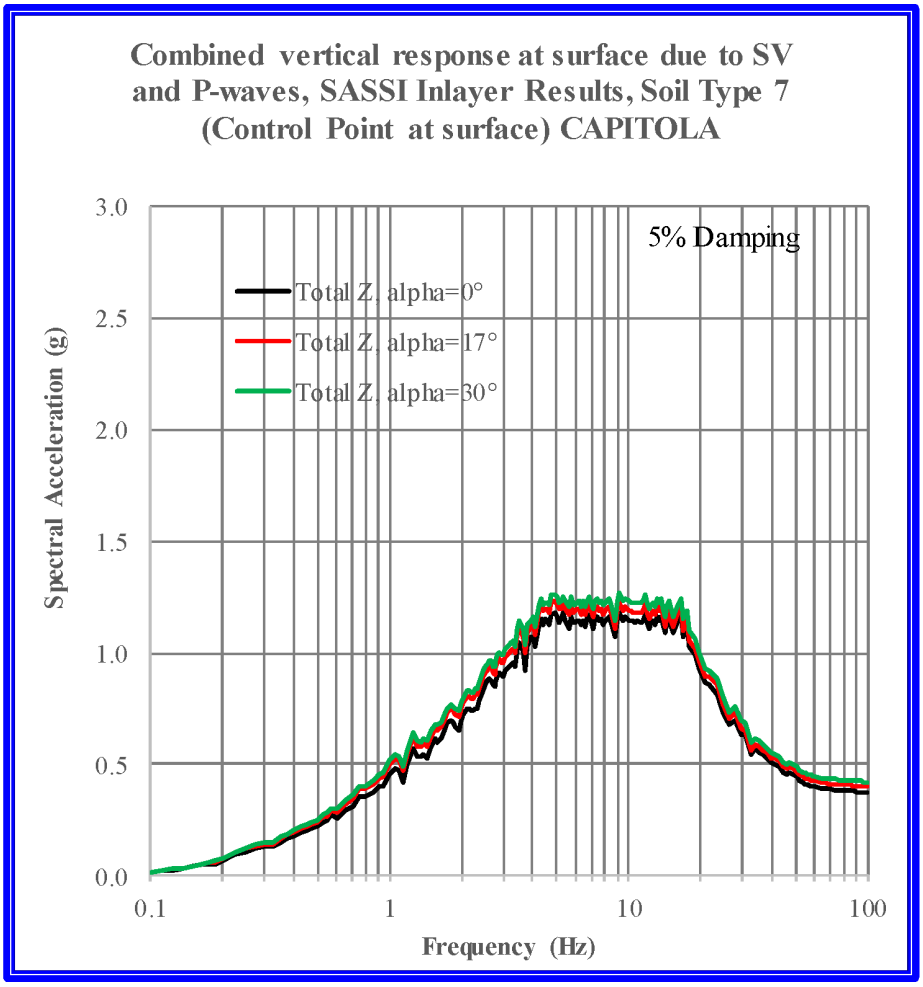

Figure 3-13. Soil Type 7 - Comparison of Combined Free-Field Vertical (Z) ARS at Surface, Capitola Input, alpha = 0°, 17°, 30°.

3.2.4 Free-Field Z-Response ARS at Depth 85′ Due to SV and P-Waves

Figure 3-14 shows the Z-response ARS at the depth of 85′ due to P-waves for α = 0°, 17°, and 30°. Note that the α = 0° curve represents the CSDRS motion (or FIRS) at this depth. The CSDRS at the rock outcrop (dashed line) is shown for reference only.

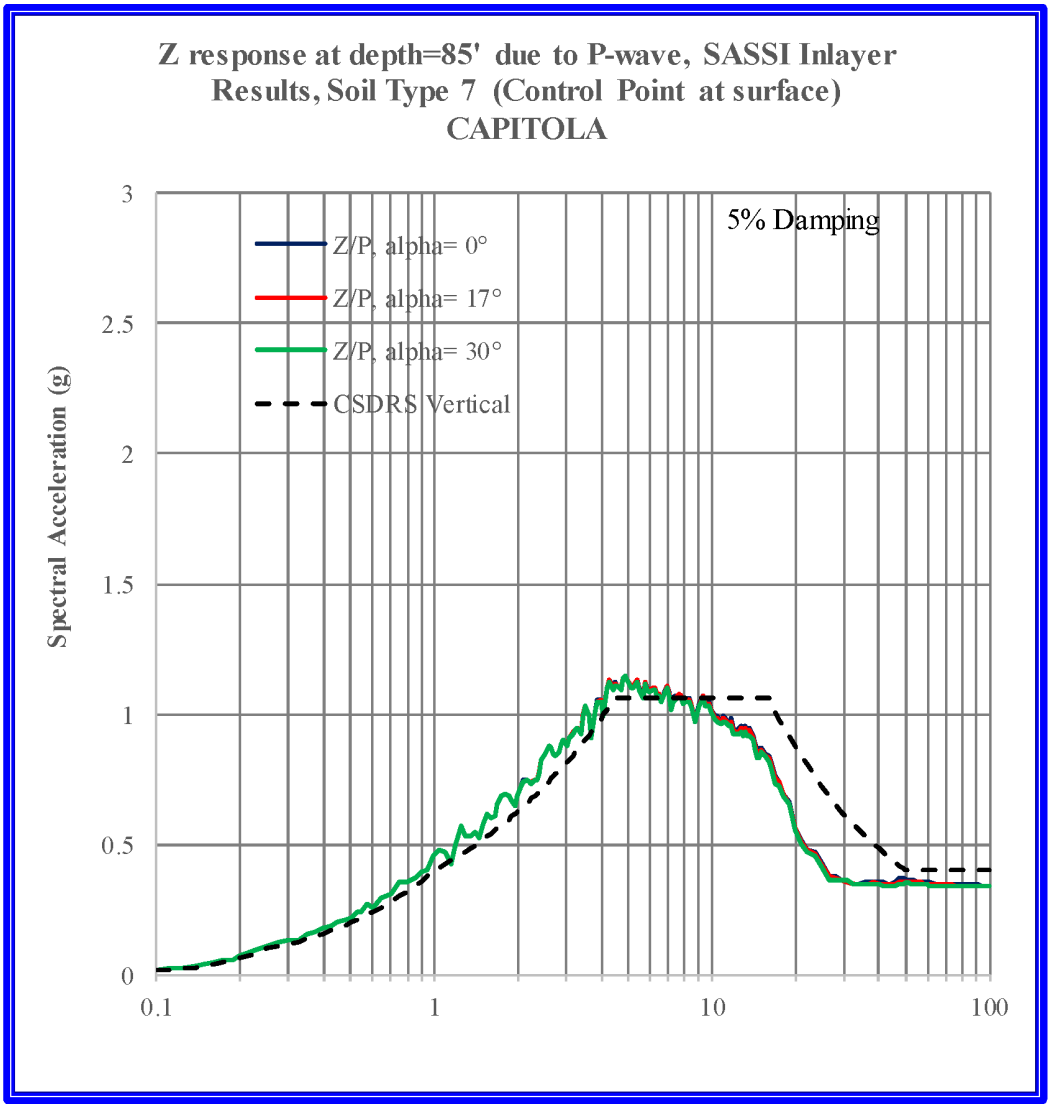

Figure 3-14. Soil Type 7 - Free-Field Uncoupled Vertical (Z) ARS at Depth=85′, Capitola Input, alpha = 0°, 17°, 30°.

Figure 3-15 shows the Z-response ARS at the depth of 85′ due to SV and P-waves for α = 17°. The combined response obtained by SRSS combination of the two curves is also shown. Also shown is the α = 0° response (solid black curve), which represents the CSDRS motion (or FIRS) at this depth. The CSDRS is exceeded by the total Z ARS.

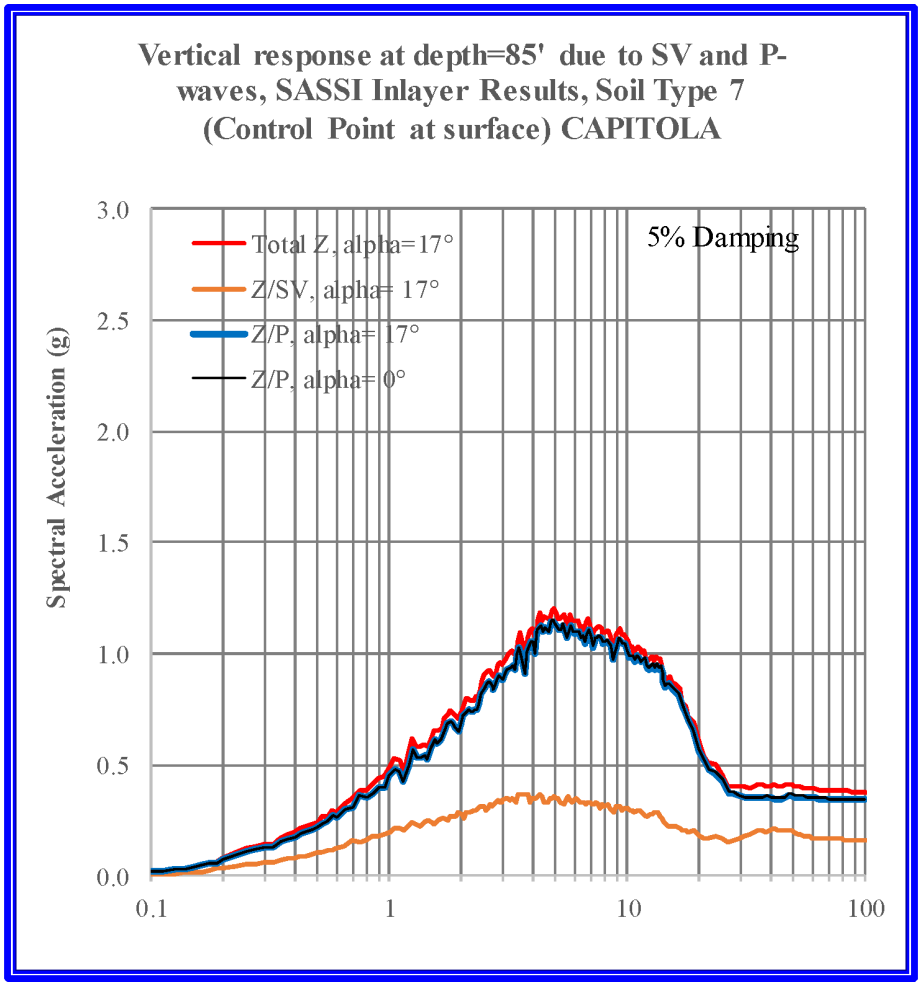

Figure 3-15. Soil Type 7 - Free-Field Vertical (Z) ARS at Depth=85′, Capitola Input, alpha = 17°.

Figure 3-16 shows the Z-response ARS at a depth of 85′ due to SV and P-waves for α = 30°. The combined response obtained by SRSS combination of the two curves is also shown. Also shown is the α = 0° response (solid black curve), which represents the CSDRS motion (or FIRS) at this depth. The CSDRS is exceeded by the total Z ARS.

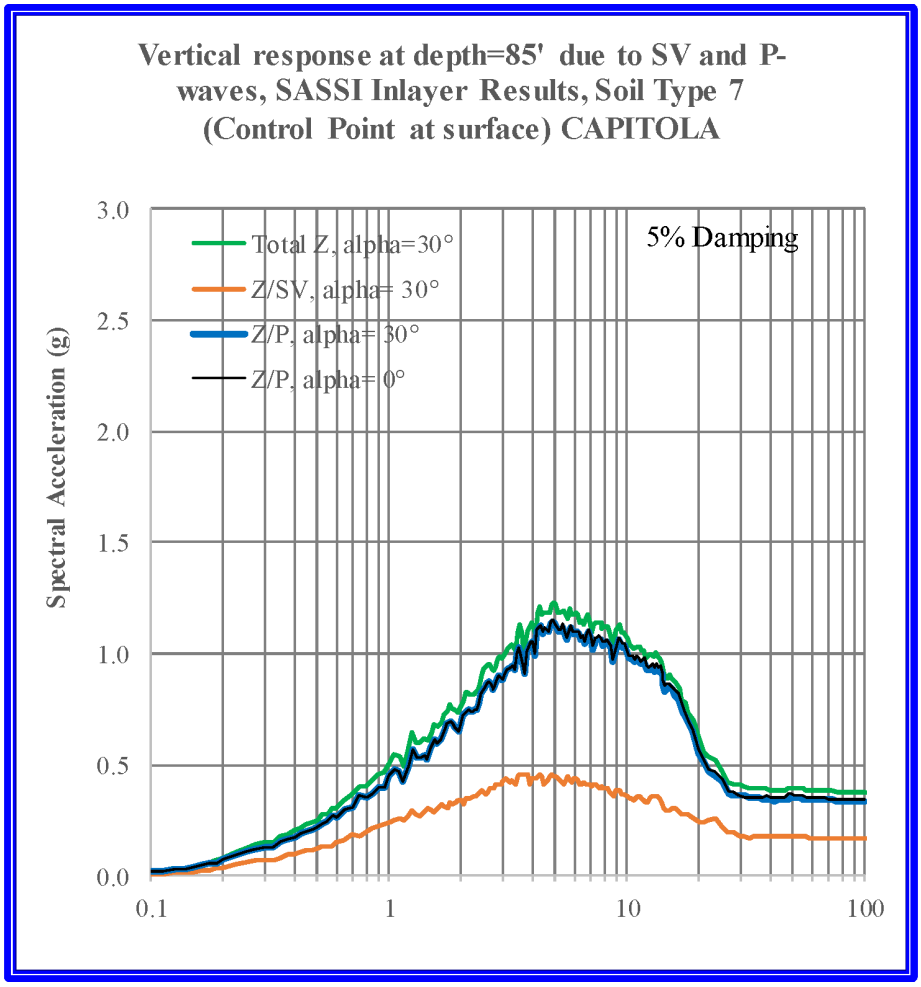

Figure 3-16. Soil Type 7 - Free-Field Vertical (Z) ARS at Depth=85′, Capitola Input, alpha = 30°.

Figure 3-17 shows a comparison of the combined Z-response ARS at a depth of 85′ for α = 0°, 17°, and 30°. Note that the α = 0° curve represents the CSDRS motion (or FIRS) at this depth. The α = 17° and α = 30° curves include the coupling term (vertical response due to SV-wave) and, thus, exceed the CSDRS that was chosen as the design basis. The motion for the α = 30° case becomes conservative when the coupling term is included.

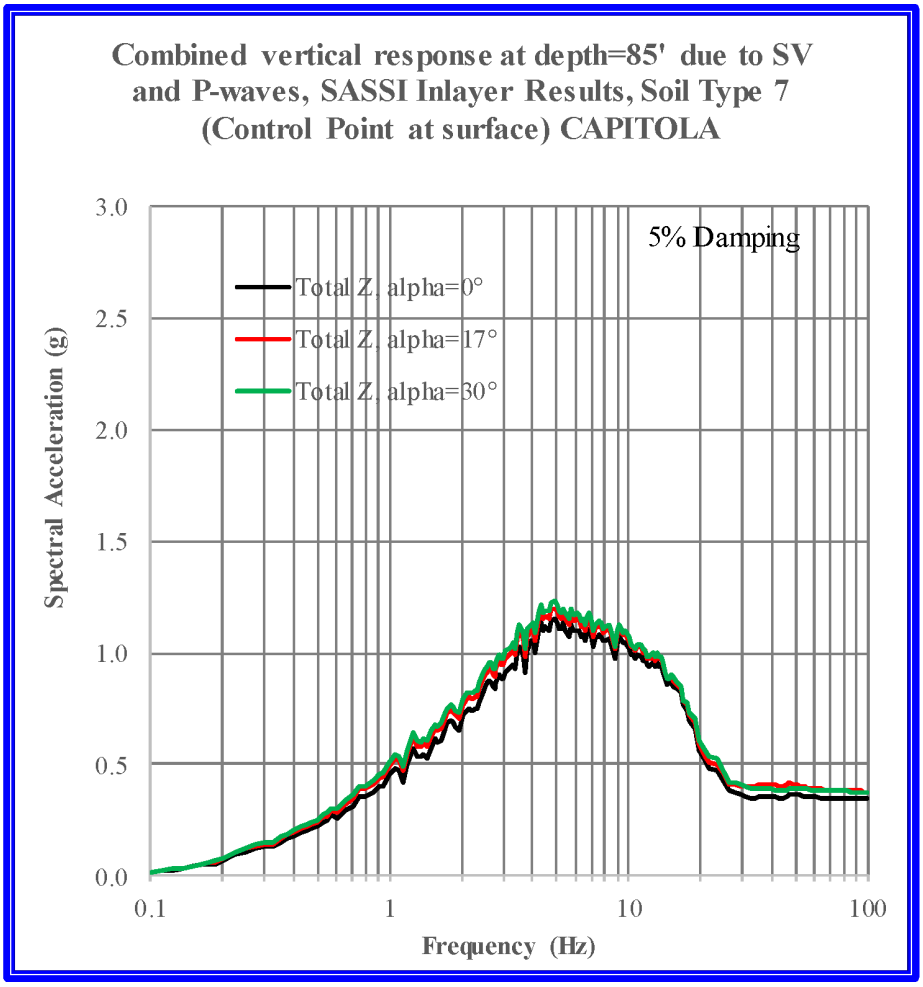

Figure 3-17. Soil Type 7 - Comparison of Combined Free-Field Vertical (Z) ARS at Depth = 85′, Capitola Input, alpha = 0°, 17°, 30°.

3.3 Discussion of Free-Field Motion

The results presented in Section 3.2 show the effect of the coupling terms due to non-vertically propagating waves. The α = 0° (vertically propagating) curves represent the CSDRS case. These results show that, even though the horizontal input motion at the surface is the same for all angles of incidence of inclined SV waves (Figure 3-2), the motion at the foundation depth exceeds those of the CSDRS (or FIRS) even without including the coupling terms from inclined waves. For example, see Figure 3-8. Once coupling terms from inclined waves are considered, the motion at the foundation depth far exceeds those of the CSDRS responses. For example, see Figure 3-9.

Therefore, the coupling terms from inclined waves should not be included in the response calculation, in order to properly maintain the as-defined, design-basis seismic inputs, the CSDRS and CSDRS-HF.

For P-waves, the vertical in-column response motion from inclined waves is close to that of the vertical motion obtained from the CSDRS when the coupling term is not considered. For example, see Figure 3-16.

4.0 SSI ANALYSIS OF RXB WITH NON-VERTICALLY PROPAGATING WAVES

This section documents the SSI analysis of the NuScale RXB subject to non-vertically propagating waves. Results in terms of in-structure response spectra (ISRS) will be compared.

The RXB is a rectangular structure, with dimensions of 346′ long, 150.5′ wide, and 167′ in height. It is embedded 86′ in the ground. An isometric view of the RXB DCA model with the surrounding backfill soil is shown in Figure 4-1. An isometric view of the north half of the RXB DCA model with the surrounding backfill soil is shown in Figure 4-2.

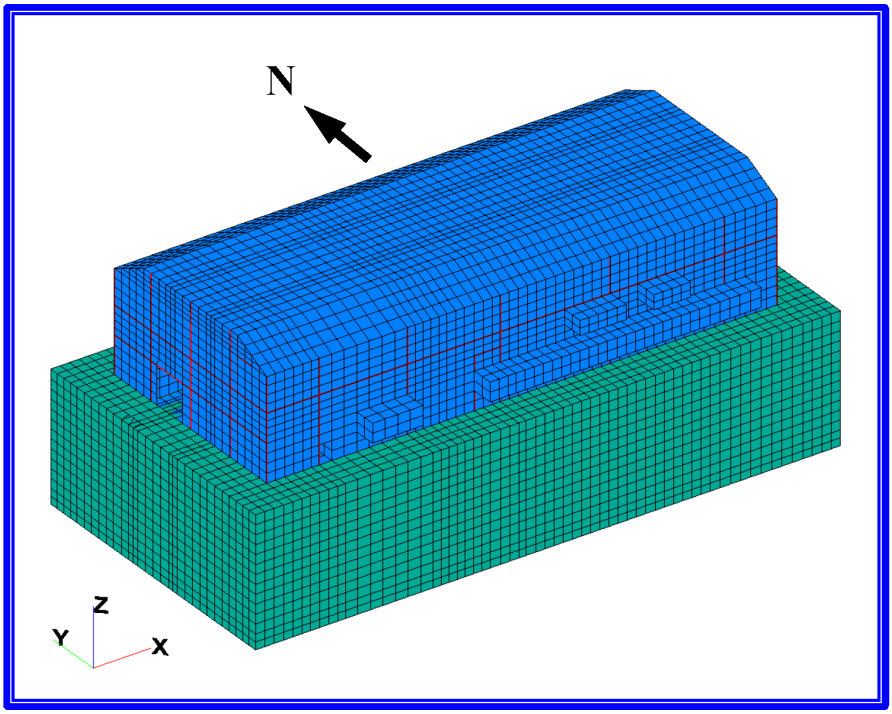

Figure 4-1. Isometric View RXB SASSI2010 Model with Backfill Soil.

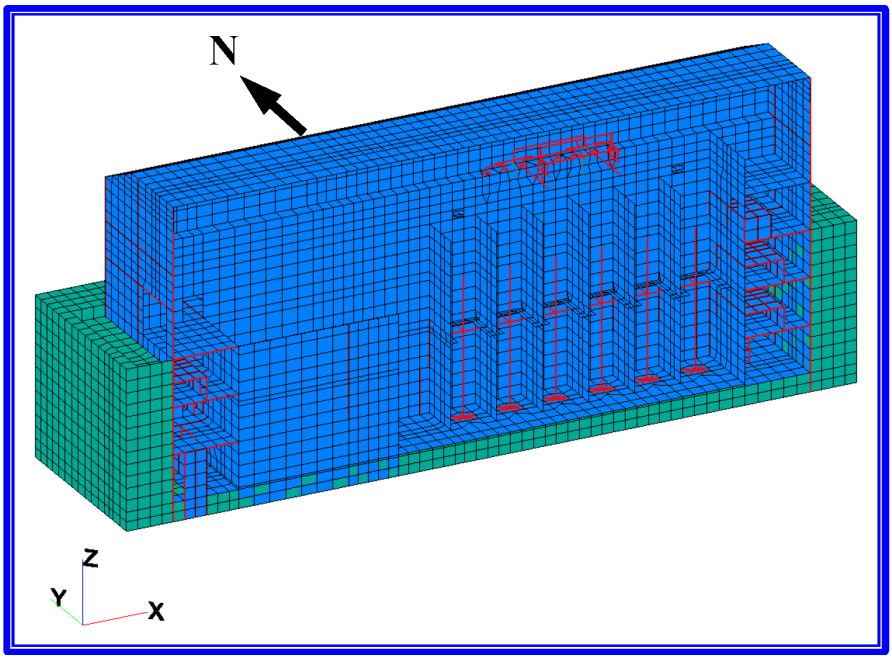

Figure 4-2. Isometric View of North Half of RXB SASSI2010 Model with Backfill Soil.

5.0 RXB ANALYSIS RESULTS FOR SOIL TYPE 7

This section provides SSI analysis results for the RXB embedded in Soil Type 7. Comparisons of ISRS due to the Capitola input propagating at various angles of incidence are presented. Based on the results discussed in Section 3.3, the uncombined ISRS are compared. Results are presented for the following three cases:

Case 1: Control point at surface, α = 0°.

Case 2: Control point at surface, α = 17°.

Case 3: Control point at surface, α = 30°.

The three cases are shown schematically in Figure 5-1.

Six locations in the RXB have been selected for ISRS comparison. The selected locations are listed in Table 5-1 and are circled in red in Figure 5-2 through Figure 5-4.The comparisons of the ISRS at the six locations are presented in Section 5.1 through Section 5.6.

The averaged-enveloped-widened ISRS at the given node from all soil cases and the cracked and uncracked models is included as a heavy, black, dashed line in each figure. Note that each averaged-enveloped-widened ISRS is the average of the combined ISRS due to 5 vertically propagating CSDRS-compatible time histories. Also, where available, the floor ISRS from the FSAR at the node elevation is included as a solid, dark-orange line.

Table 5-1. Locations for ISRS Comparison.

Item No.	Single Bldg. Node No.	X (East) (in)	Y (North) (in)	Z (Vert) (in)	Description
1	3996	0	873	120	El. 24′, Top of Basemat, NW Corner
2	5642	4092	873	120	El. 24′, Top of Basemat, NE Corner
3	22810	0	-873	1020	El.100′, SW Corner
4	22994	420	-453	1020	El. 100', Spent Fuel Pool, SW Corner
5	29098	0	873	1824	El. 167′, Roof, NW Corner
6	30350	2019.5	0	1980	El. 181′, Roof, Center

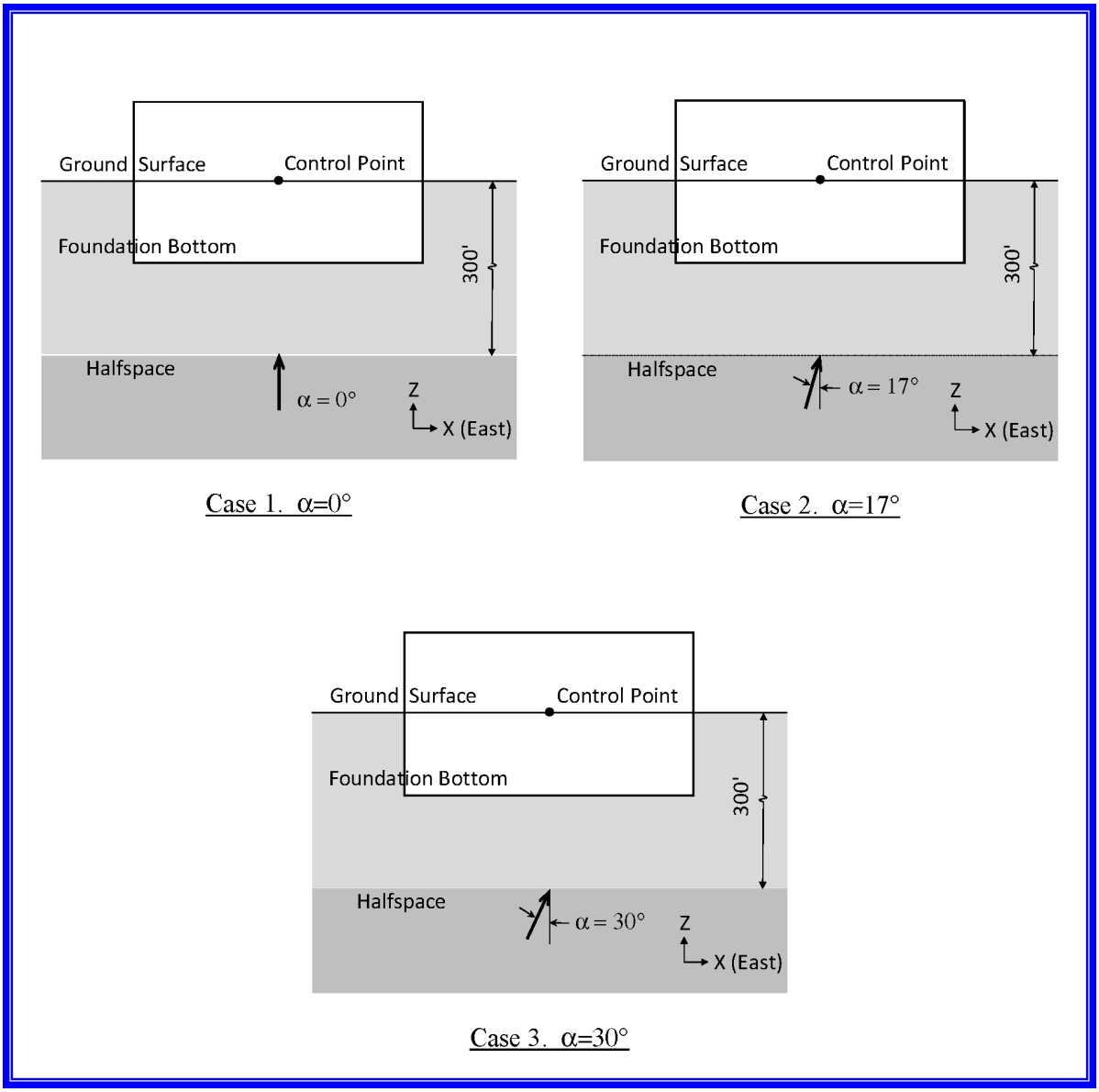

Figure 5-1. RXB Analysis Cases.

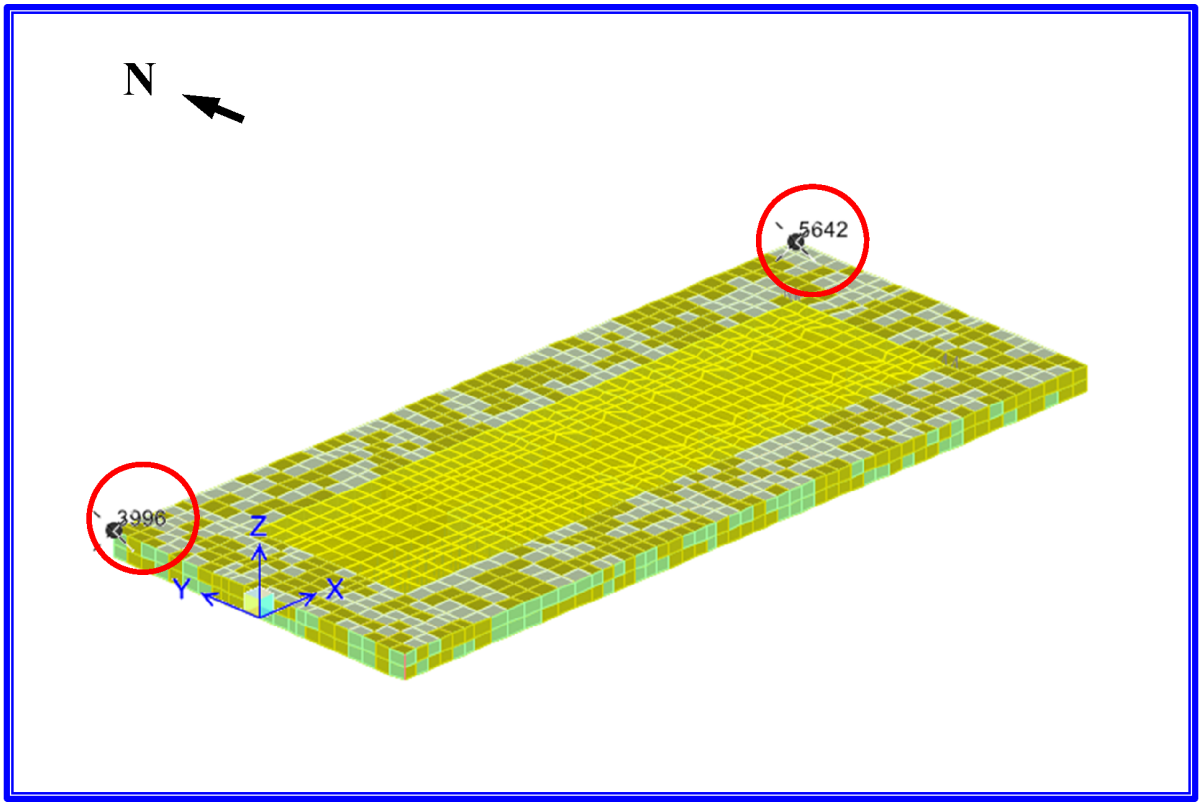

Figure 5-2. Selected RXB Nodes for ISRS Comparison at Top of Basemat.

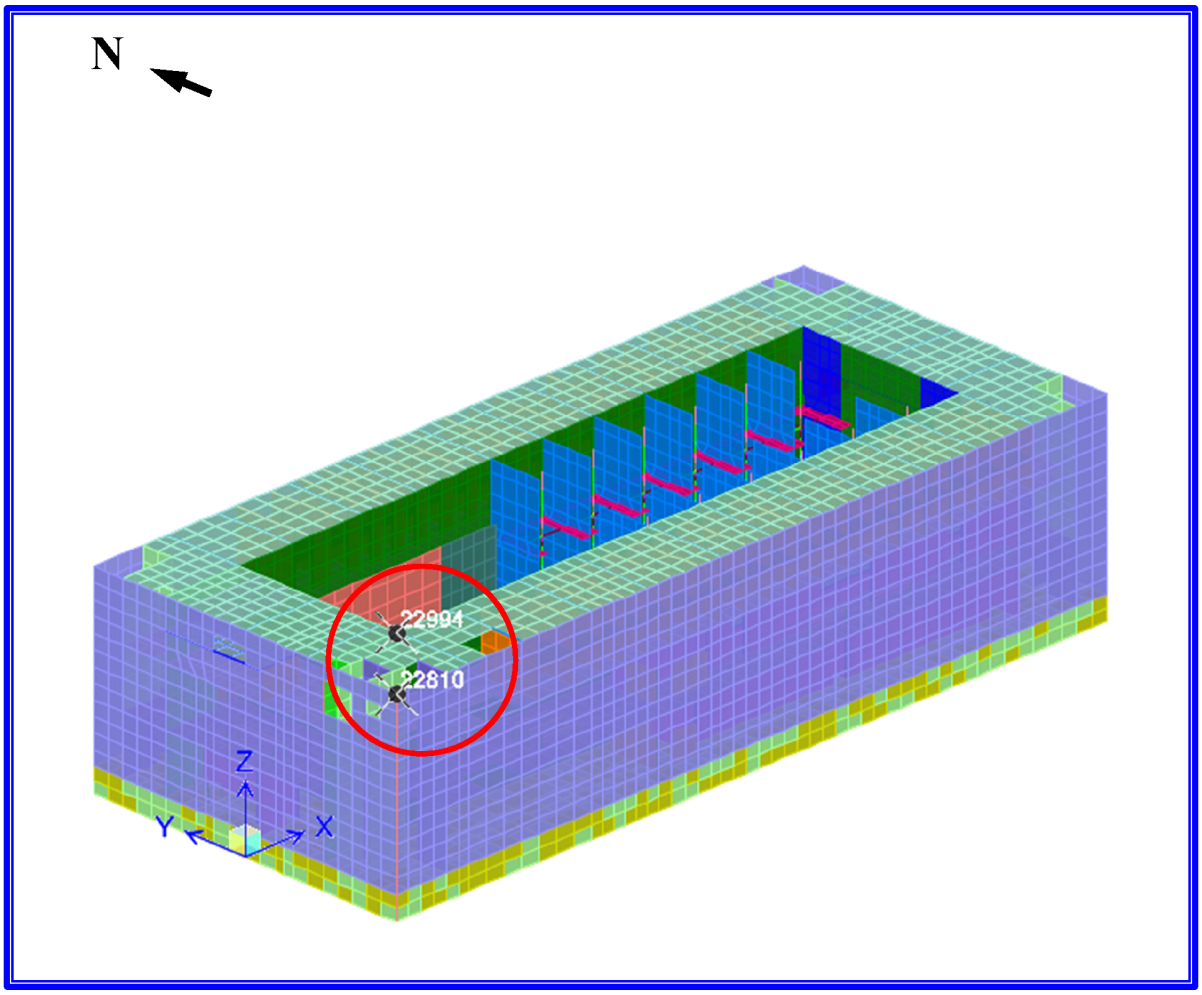

Figure 5-3. Selected RXB Nodes for ISRS Comparison at El. 100′.

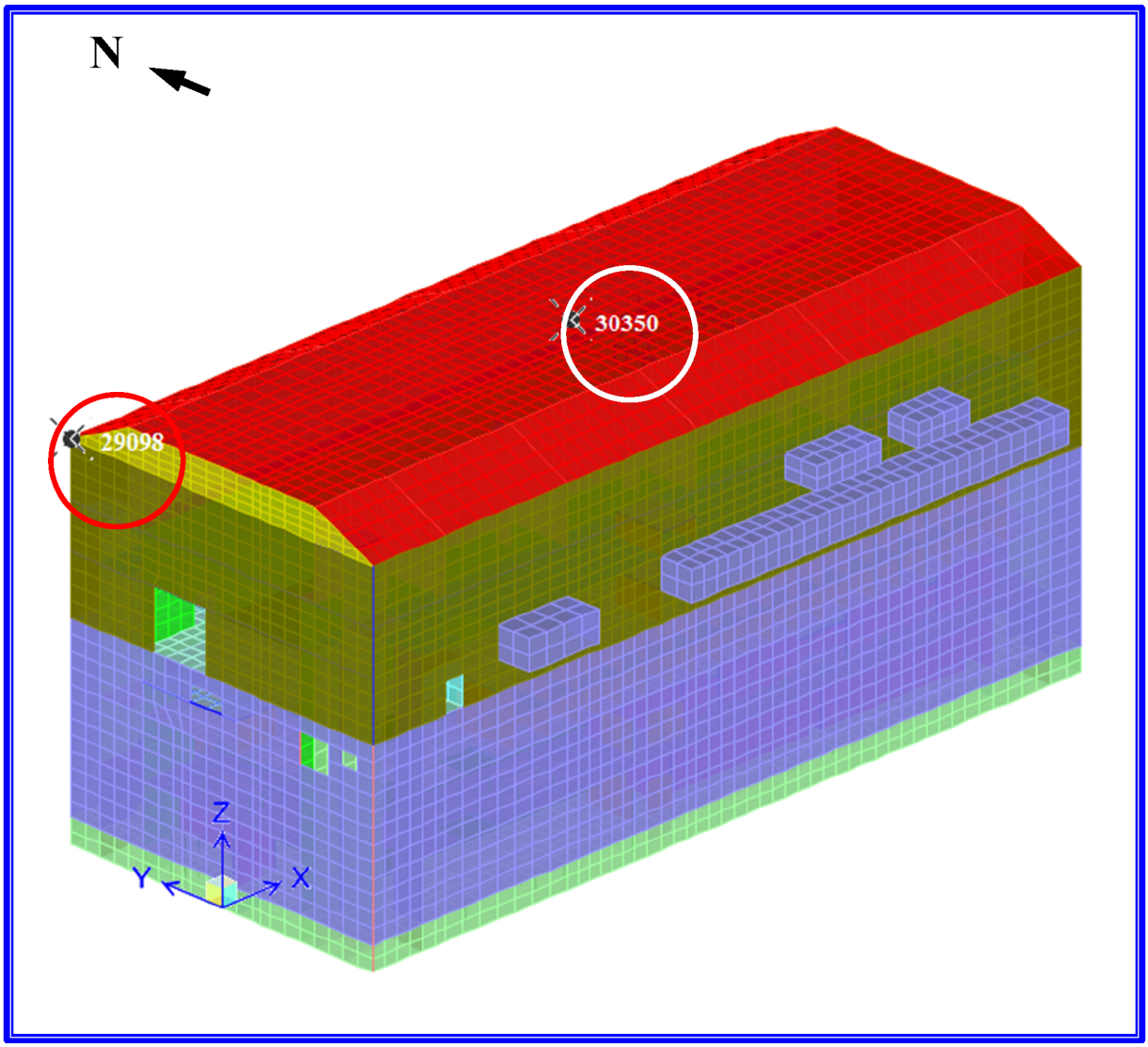

Figure 5-4. Selected RXB Nodes for ISRS Comparison at Roof.

5.1 Comparison of Uncombined ISRS at Node 3996 (Top of Basemat, NW Corner)

This section presents comparisons of the uncombined ISRS at Node 3996 (El. 24′-0″, top of basemat, northwest corner). Note that the α=0° curve represents the response to the CSDRS motion. The α=0°, α=17°, and α=30° curves do not include the coupling terms. Also note that the CSDRS at rock outcrop (thin dashes) is shown for reference only. In Figure 5-5, the α=17° curve is enveloped by the floor ISRS, except for a band from 50 to 60 Hz. The α=30° curve is enveloped by the floor ISRS, except for a band from 3.5 to 4.5 Hz, from 6 Hz to 11 Hz, and from 40 Hz to 100 Hz. When the average ISRS of the five time histories is used, the exceedances are expected to be smaller.

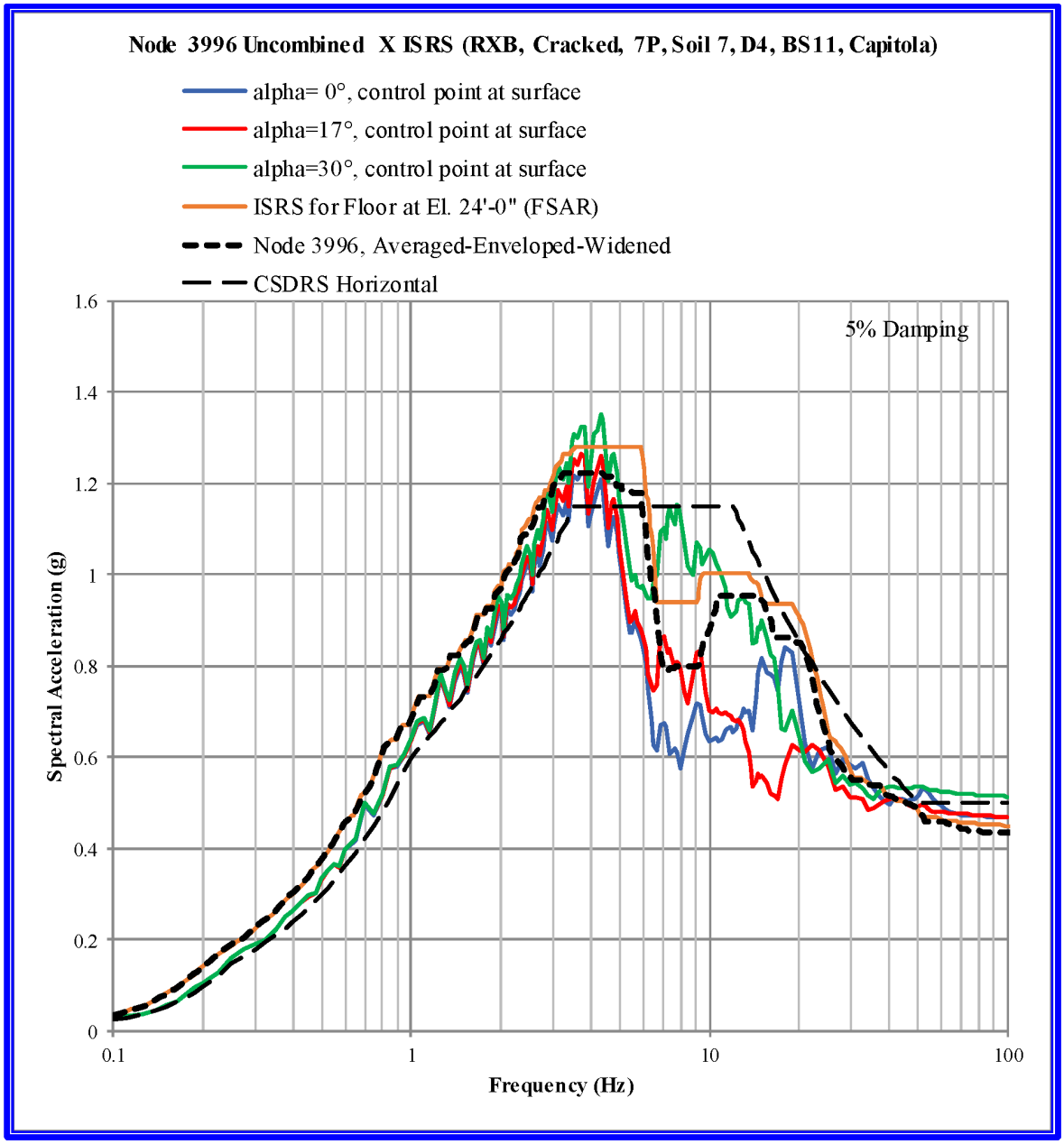

Figure 5-5. RXB - Uncombined East-West (X) ISRS, Node 3996, El. 24'-0", Top of Basemat, NW Corner, Capitola Input.

In Figure 5-6, the floor ISRS curve envelopes the α=17° and α=30° curves, except for a peak at about 1.3 Hz and a band from 4.5 Hz to 6 Hz. When the average ISRS of the five time histories is used, the exceedances are expected to be smaller.

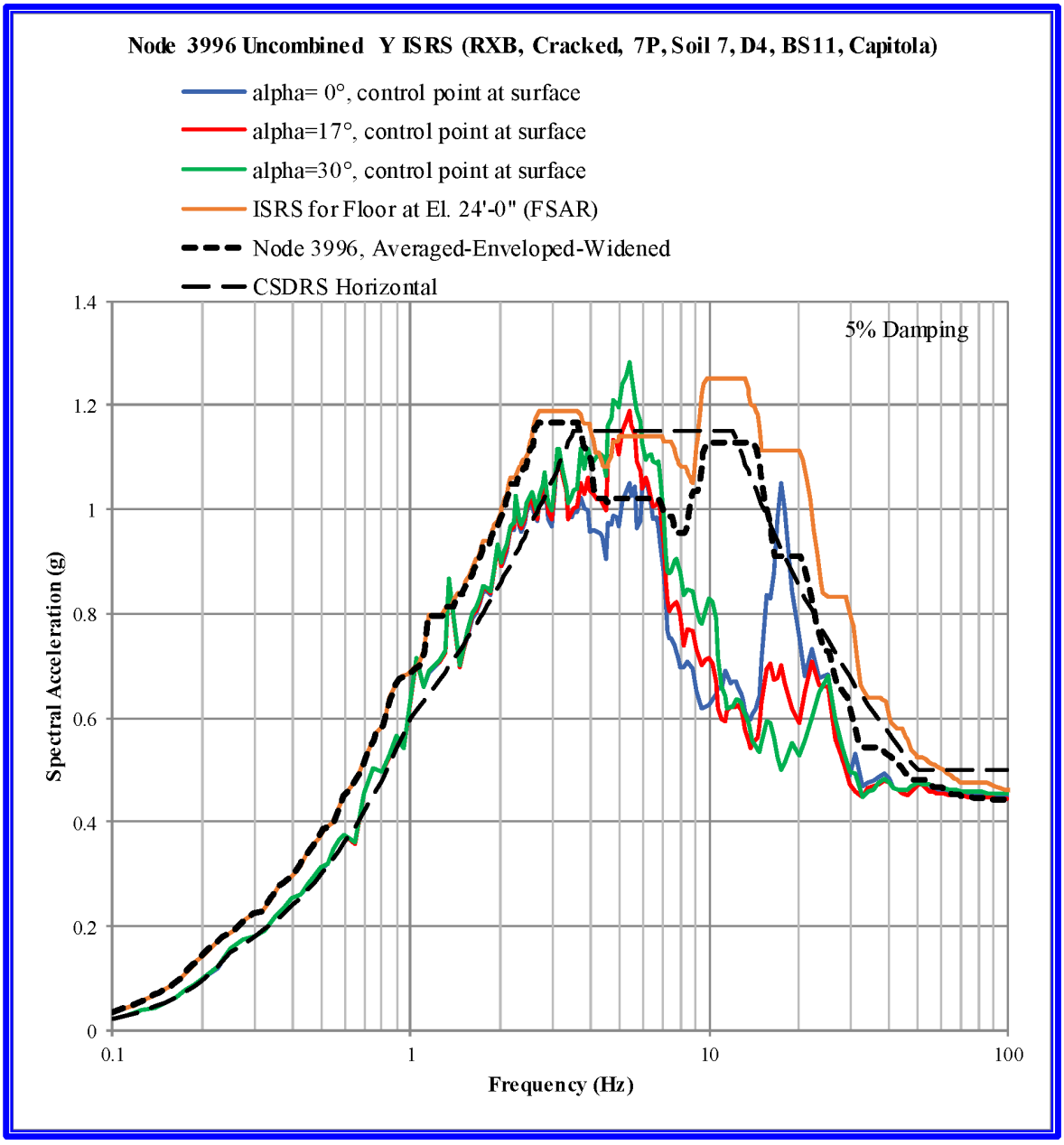

Figure 5-6. RXB - Uncombined North-South (Y) ISRS, Node 3996, El. 24'-0"Top of Basemat, NW Corner, Capitola Input.

In Figure 5-7, the floor ISRS curve envelopes the α=17° and α=30° curves.

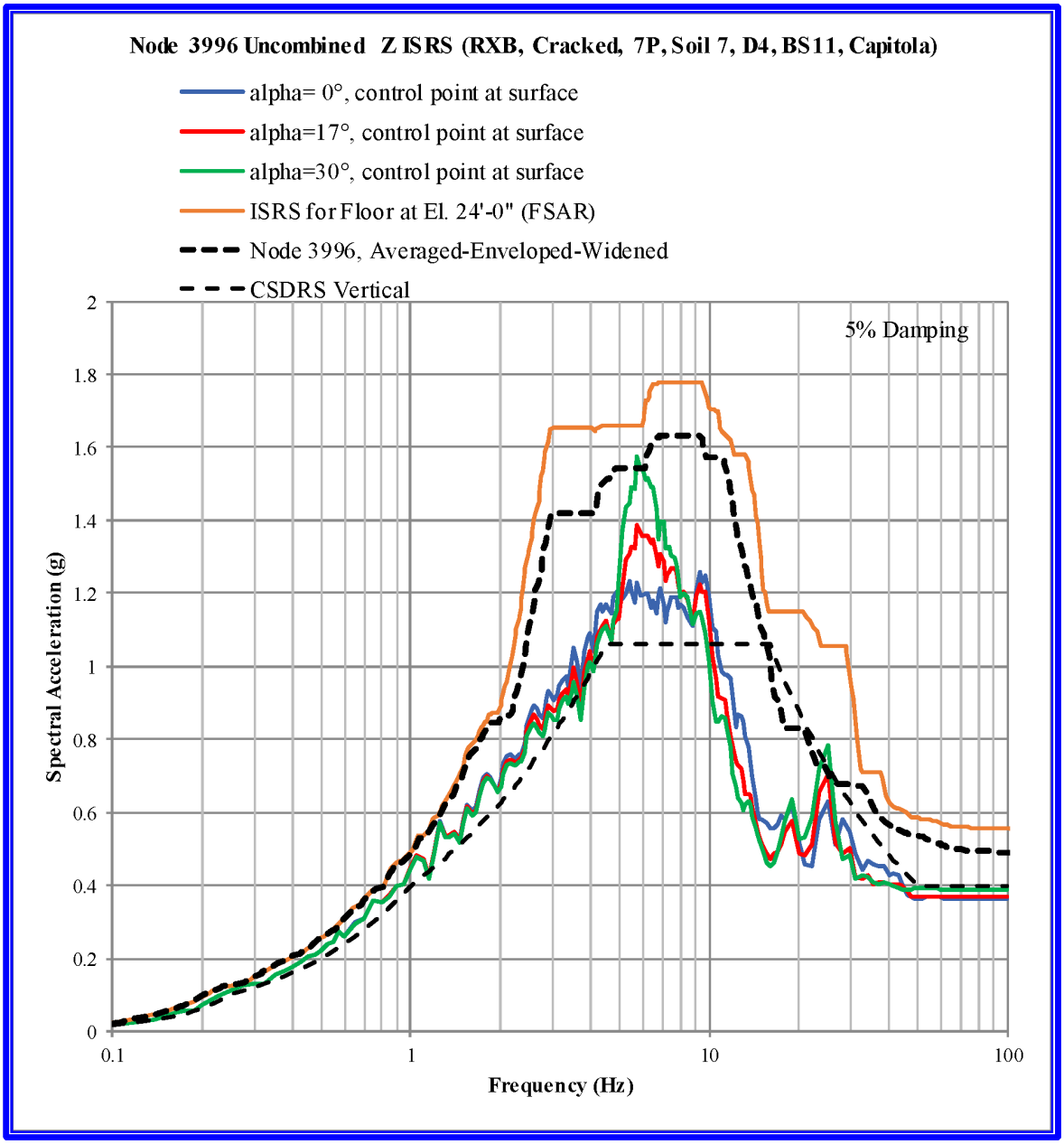

Figure 5-7. RXB - Uncombined Vertical (Z) ISRS, Node 3996, El. 24'-0"Top of Basemat, NW Corner, Capitola Input.

5.2 Comparison of Uncombined ISRS at Node 5642 (Top of Basemat, NE Corner)

This section presents comparisons of the uncombined ISRS at Node 5642 (top of basemat, northeast corner). Note that the α=0° curve represents the response to the CSDRS motion. The

α=0°, α=17°, and α=30° curves do not include the coupling terms. Also note that the CSDRS at rock outcrop (thin dashes) is shown for reference only..

In Figure 5-8, the α=17° curve is enveloped by the floor ISRS. The α=30° curve is enveloped by the floor ISRS, except for a band from 3.5 to 6 Hz, and from 35 Hz to 100 Hz. When the average ISRS of the five time histories is used, the exceedances are expected to be smaller.

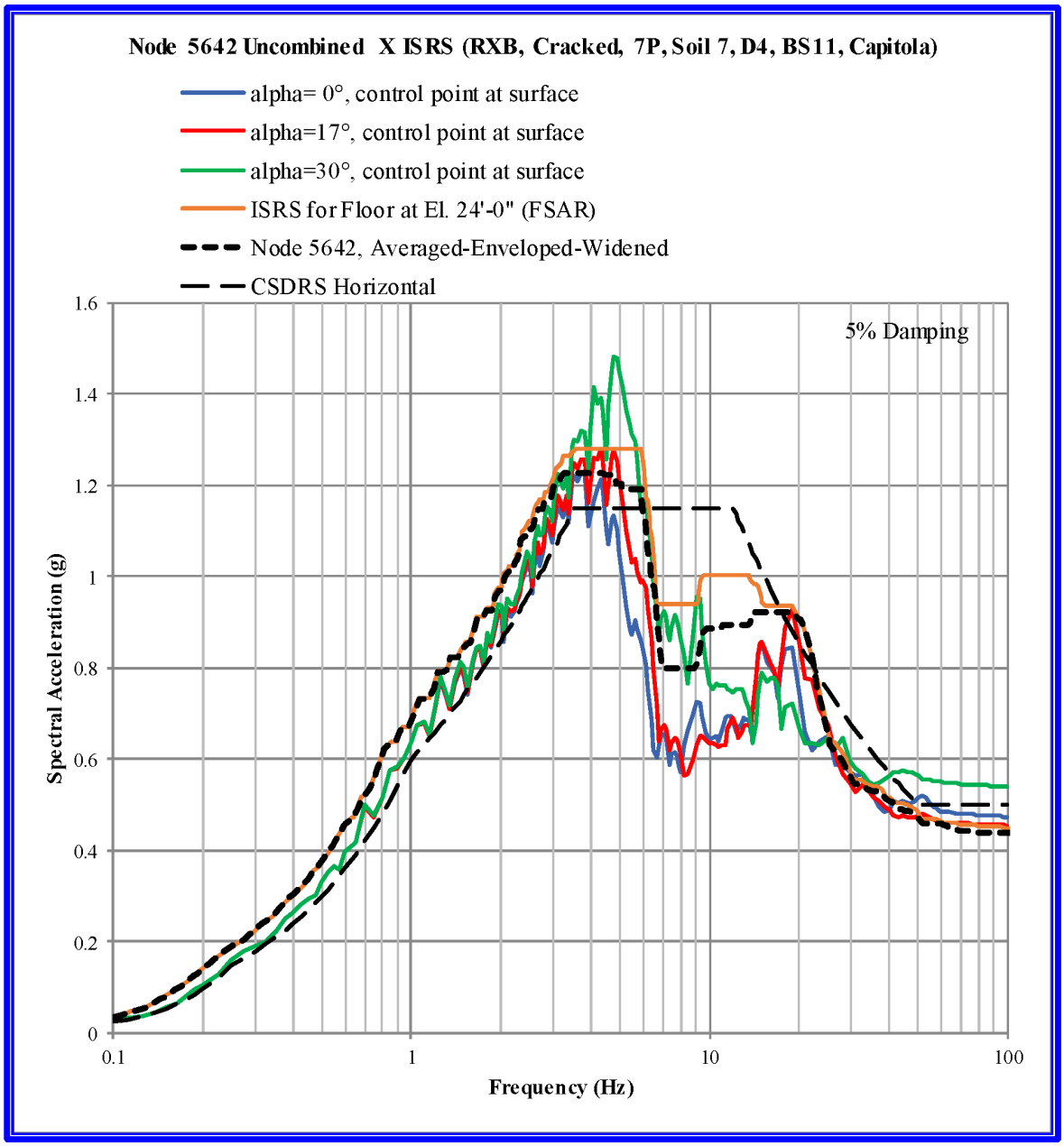

Figure 5-8. RXB - Uncombined East-West (X) ISRS, Node 5642, El. 24'-0" Top of Basemat, NE Corner, Capitola Input.

In Figure 5-9, the floor ISRS curve envelopes the α=17° and α=30° curves, except for a peak at about 1.3 Hz and from 50 Hz to 100 Hz. When the average ISRS of the five time histories is used, the exceedances are expected to be smaller.

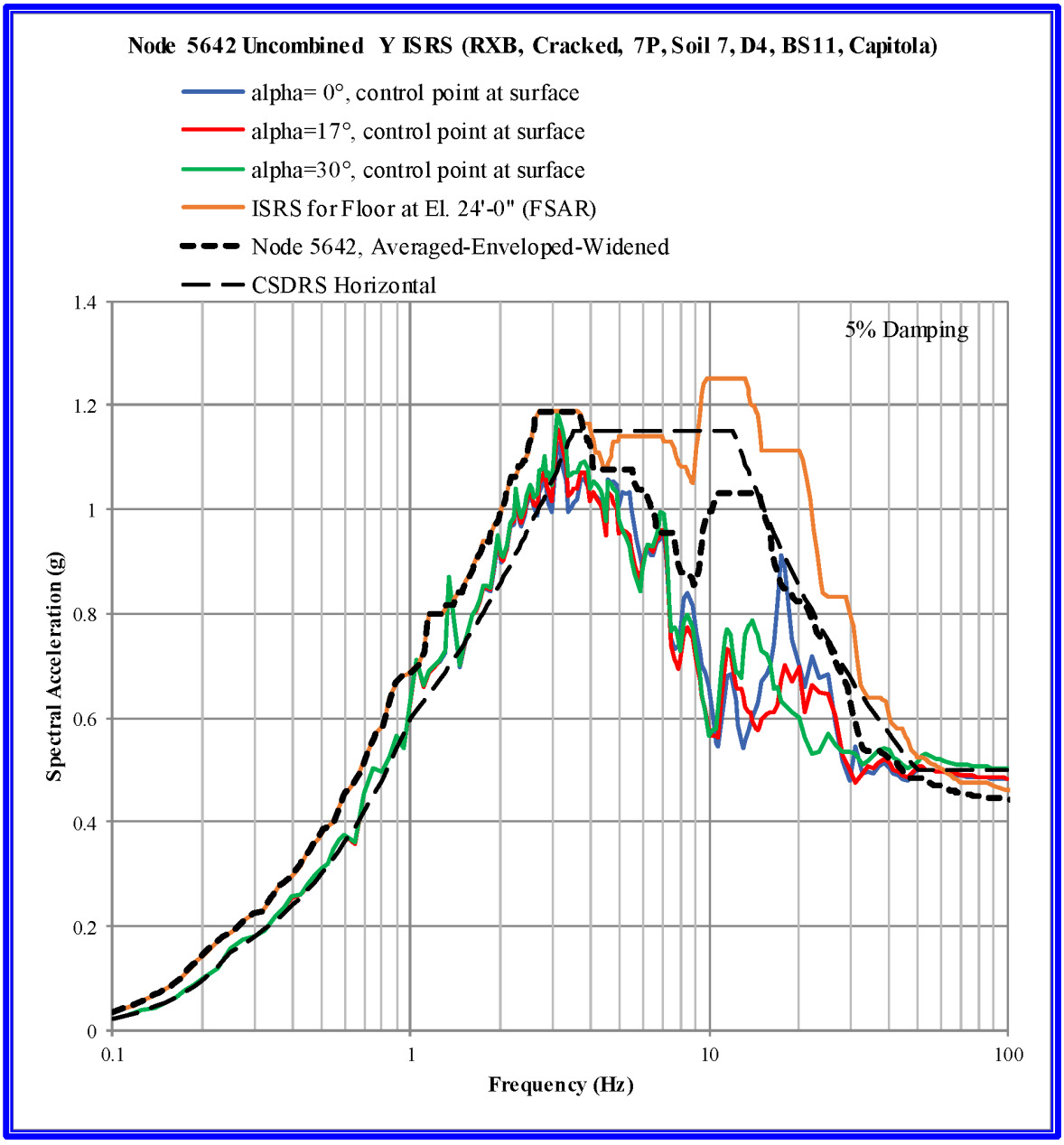

Figure 5-9. RXB - Uncombined North-South (Y) ISRS, Node 5642, El. 24'-0", Top of Basemat, NE Corner, Capitola Input.

In Figure 5-10, the floor ISRS curve envelopes the α=17° and α=30° curves.

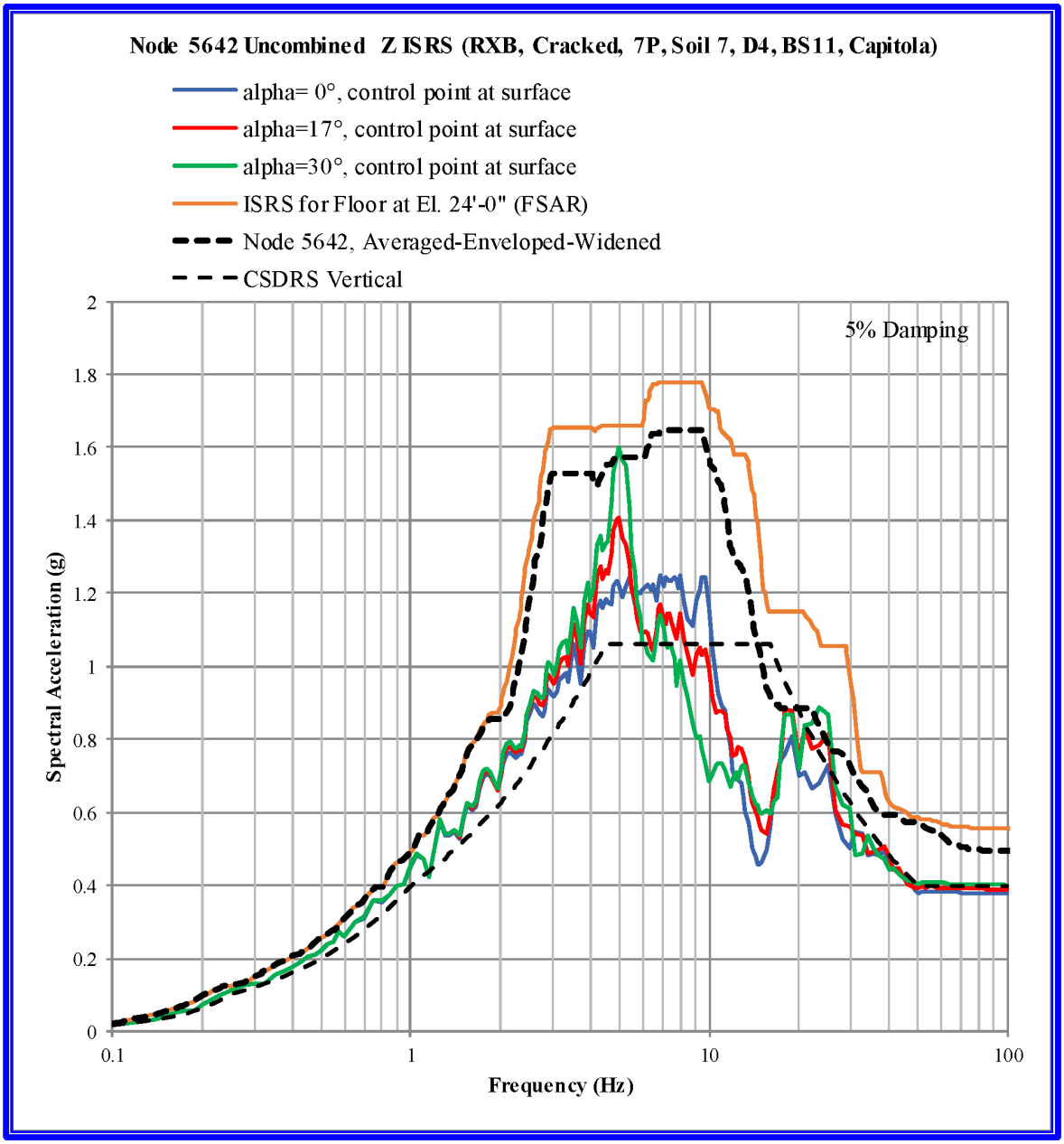

Figure 5-10. RXB - Uncombined Vertical (Z) ISRS, Node 5642, El. 24'-0", Top of Basemat, NE Corner, Capitola Input.

5.3 Comparison of Uncombined ISRS at Node 22810 (El. 100′, SW Corner)

This section presents comparisons of the uncombined ISRS at Node 22810 (El. 100′, southwest corner). Note that the α=0° curve represents the response to the CSDRS motion. The α=0°,

α=17°, and α=30° curves do not include the coupling terms. Also note that the CSDRS at rock outcrop (thin dashes) is shown for reference only.

In Figure 5-11, the floor ISRS curve envelopes the α=17° and α=30° curves.

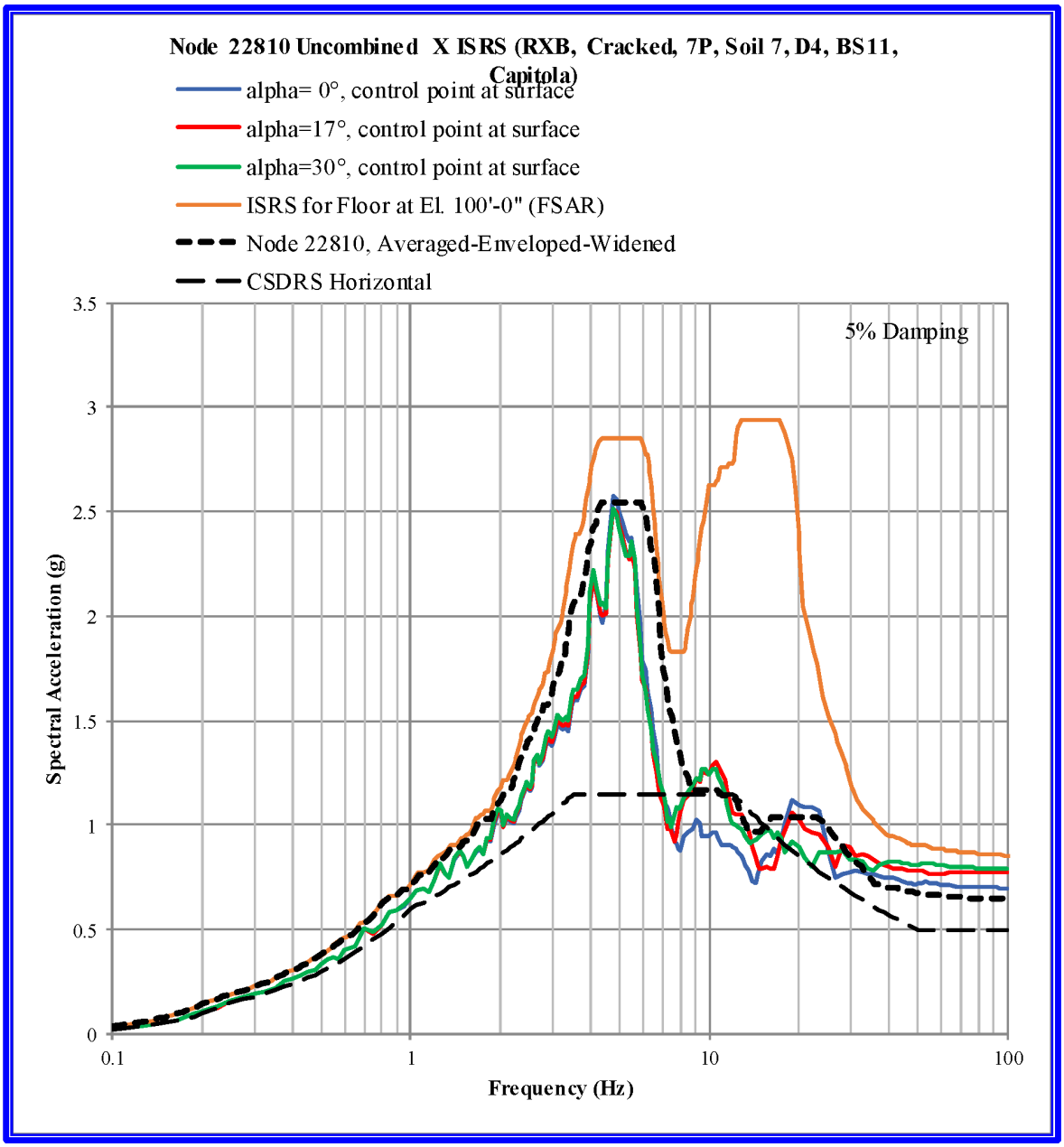

Figure 5-11. RXB - Uncombined East-West (X) ISRS, Node 22810, El. 100', SW Corner, Capitola Input.

In Figure 5-12, the floor ISRS curve envelopes the α=17° and α=30° curves.

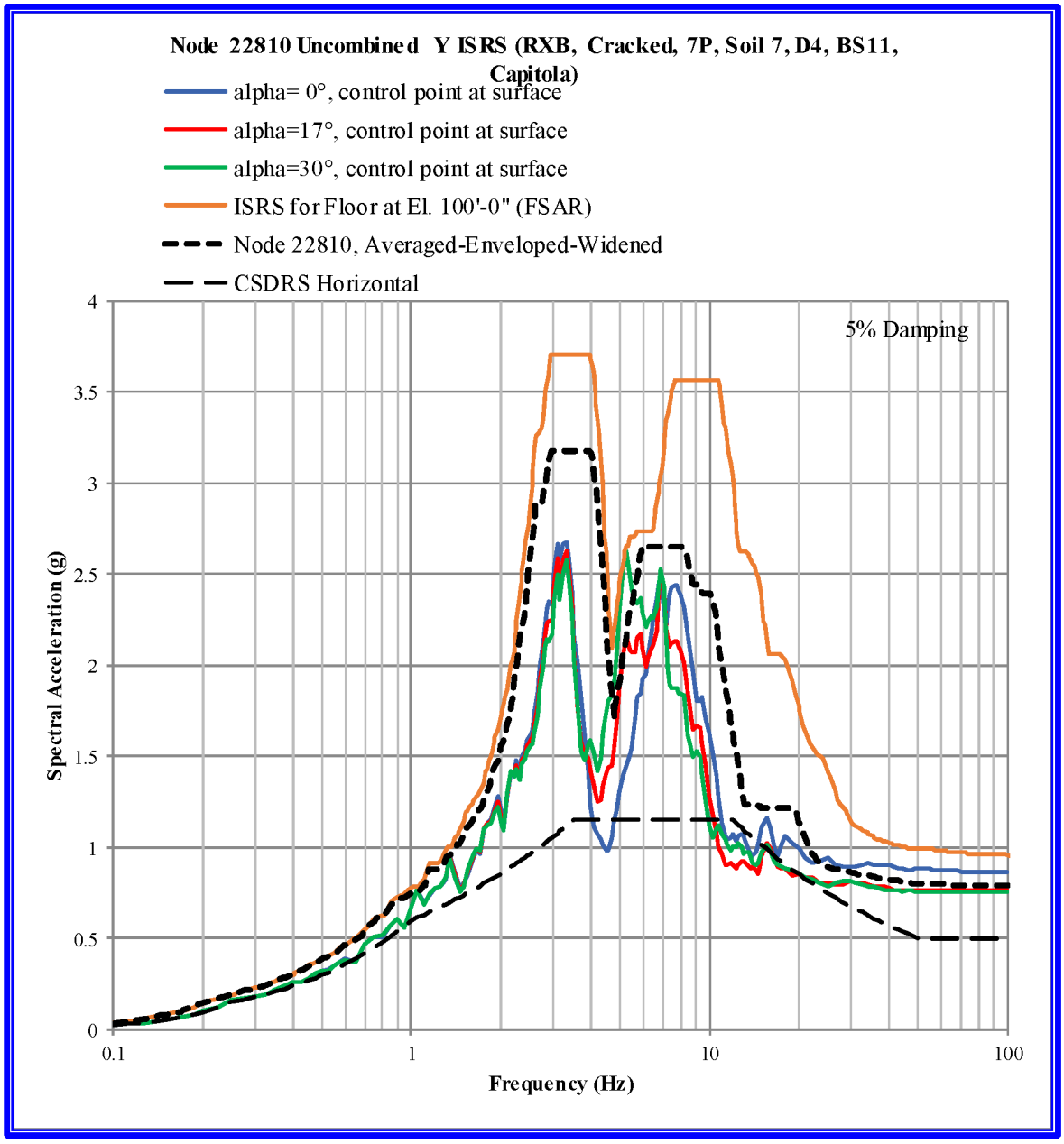

Figure 5-12. RXB - Uncombined North-South (Y) ISRS, Node 22810, El. 100', SW Corner, Capitola Input.

In Figure 5-13, the floor ISRS curve envelopes the α=17° and α=30° curves.

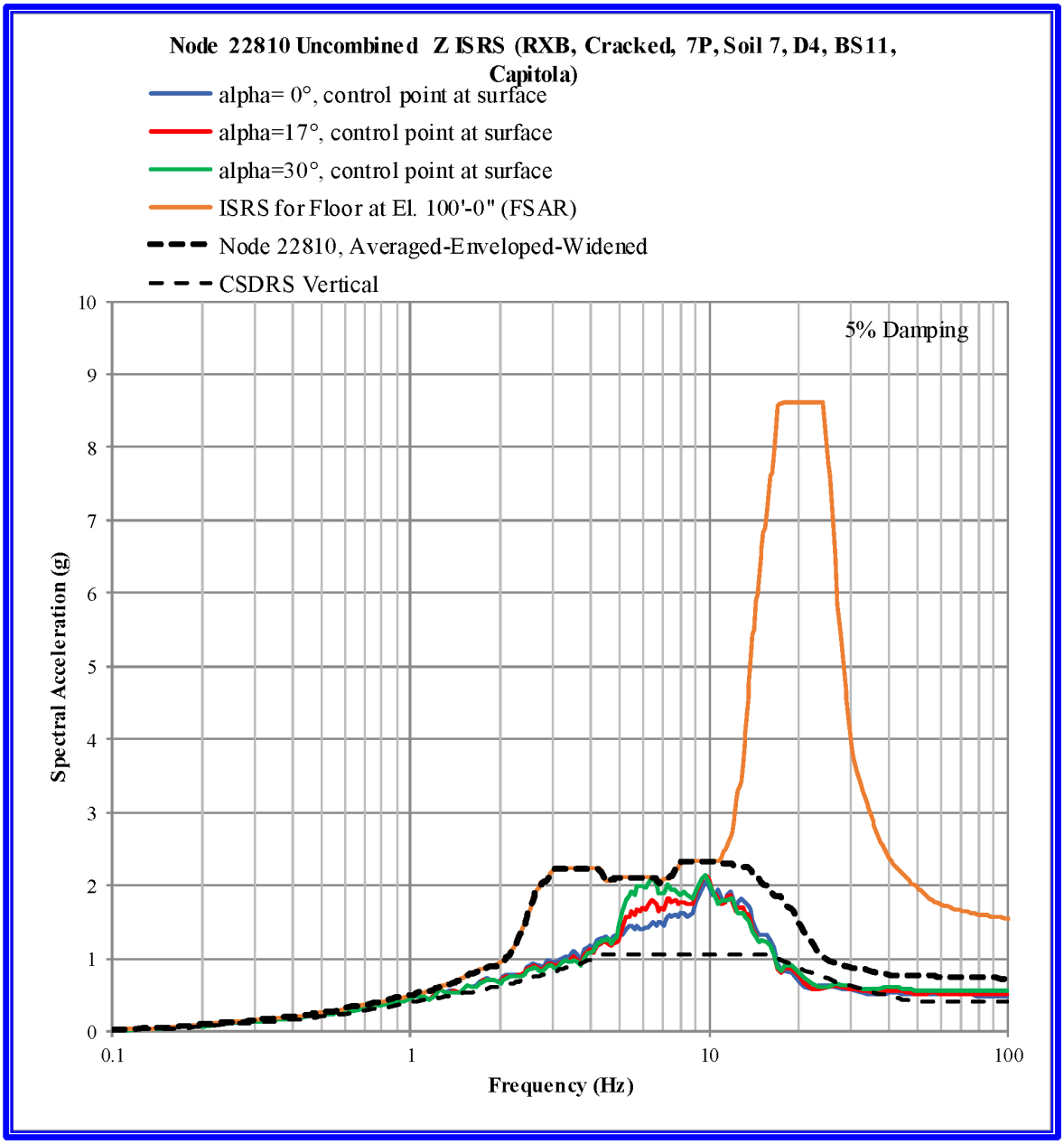

Figure 5-13. RXB - Uncombined Vertical (Z) ISRS, Node 22810, El. 100', SW Corner, Capitola Input.

5.4 Comparison of Uncombined ISRS at Node 22994 (El. 100′, SFP, SW Corner)

This section presents comparisons of the uncombined ISRS at Node 22994 (El. 100′, southwest corner). Note that the α=0° curve represents the response to the CSDRS motion. The α=0°,

α=17°, and α=30° curves do not include the coupling terms. Also note that the CSDRS at rock outcrop (thin dashes) is shown for reference only.

In Figure 5-14, the floor ISRS curve envelopes the α=17° and α=30° curves.

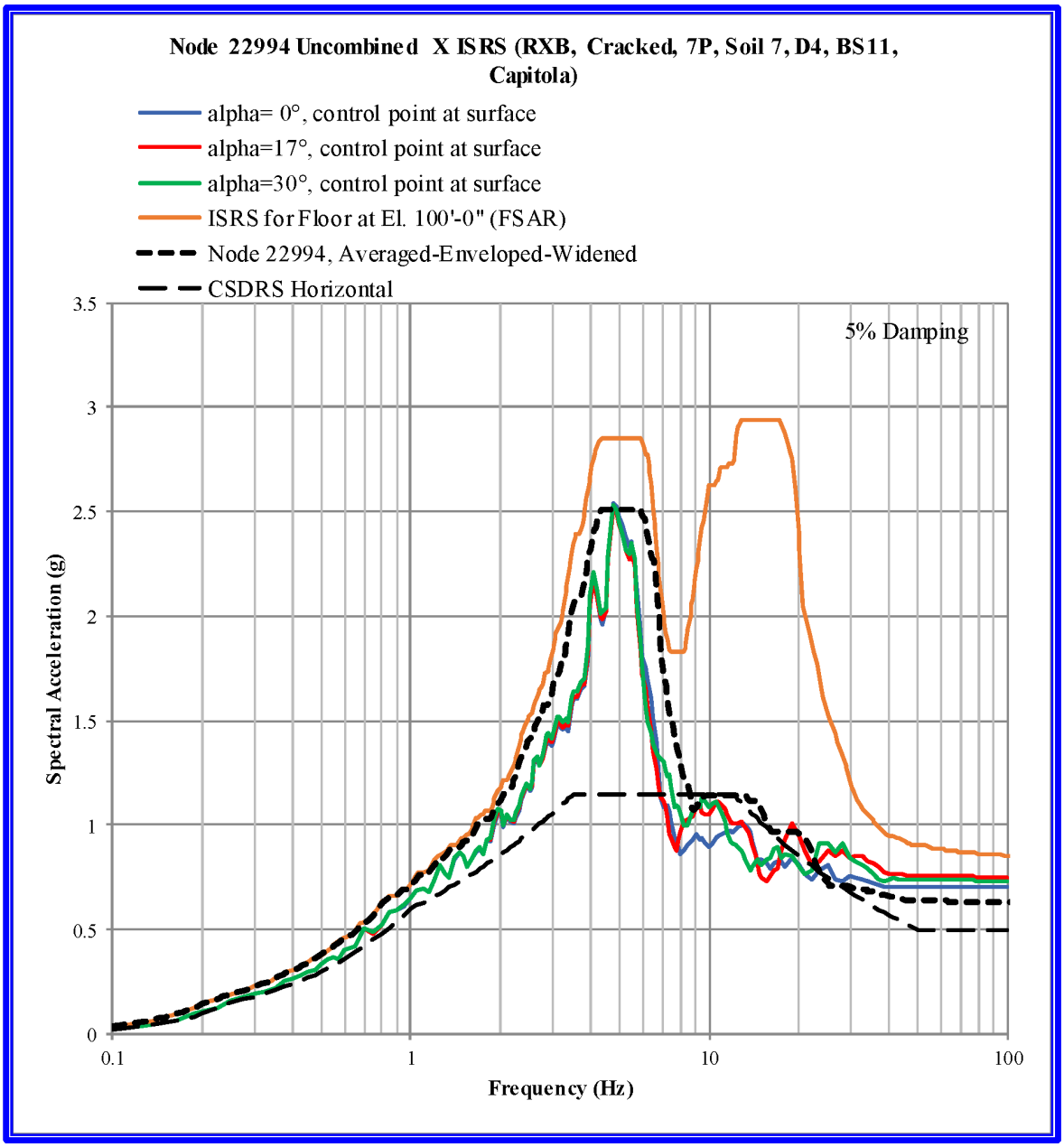

Figure 5-14. RXB - Uncombined East-West (X) ISRS, Node 22994, El. 100′, Spent Fuel Pool, SW Corner, Capitola Input.

In Figure 5-15, the floor ISRS curve envelopes the α=17° and α=30° curves.

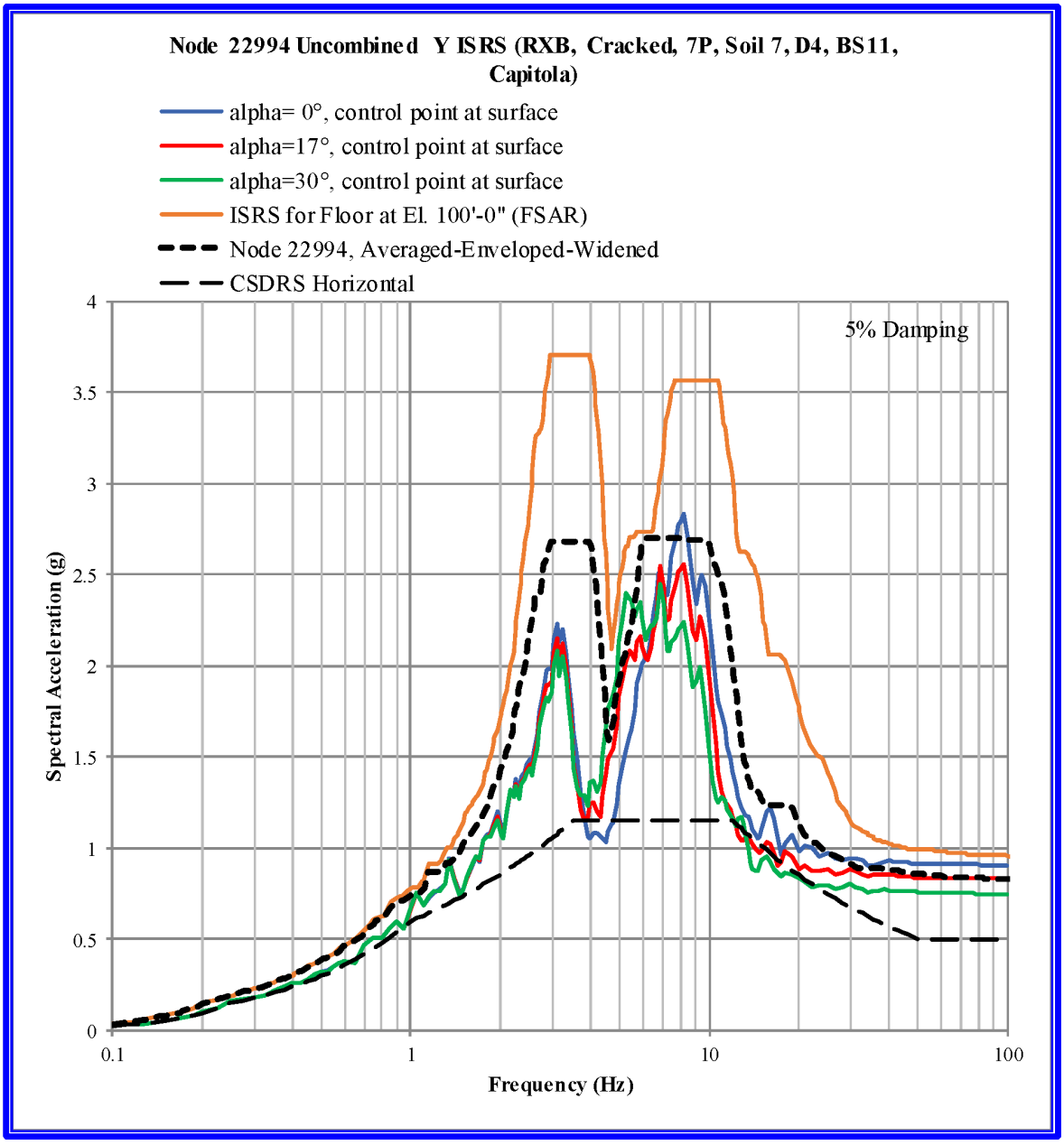

Figure 5-15. RXB - Uncombined North-South (Y) ISRS, Node 22994, El. 100′, Spent Fuel Pool, SW Corner, Capitola Input.

In Figure 5-16, the floor ISRS curve envelopes the α=17° and α=30° curves.

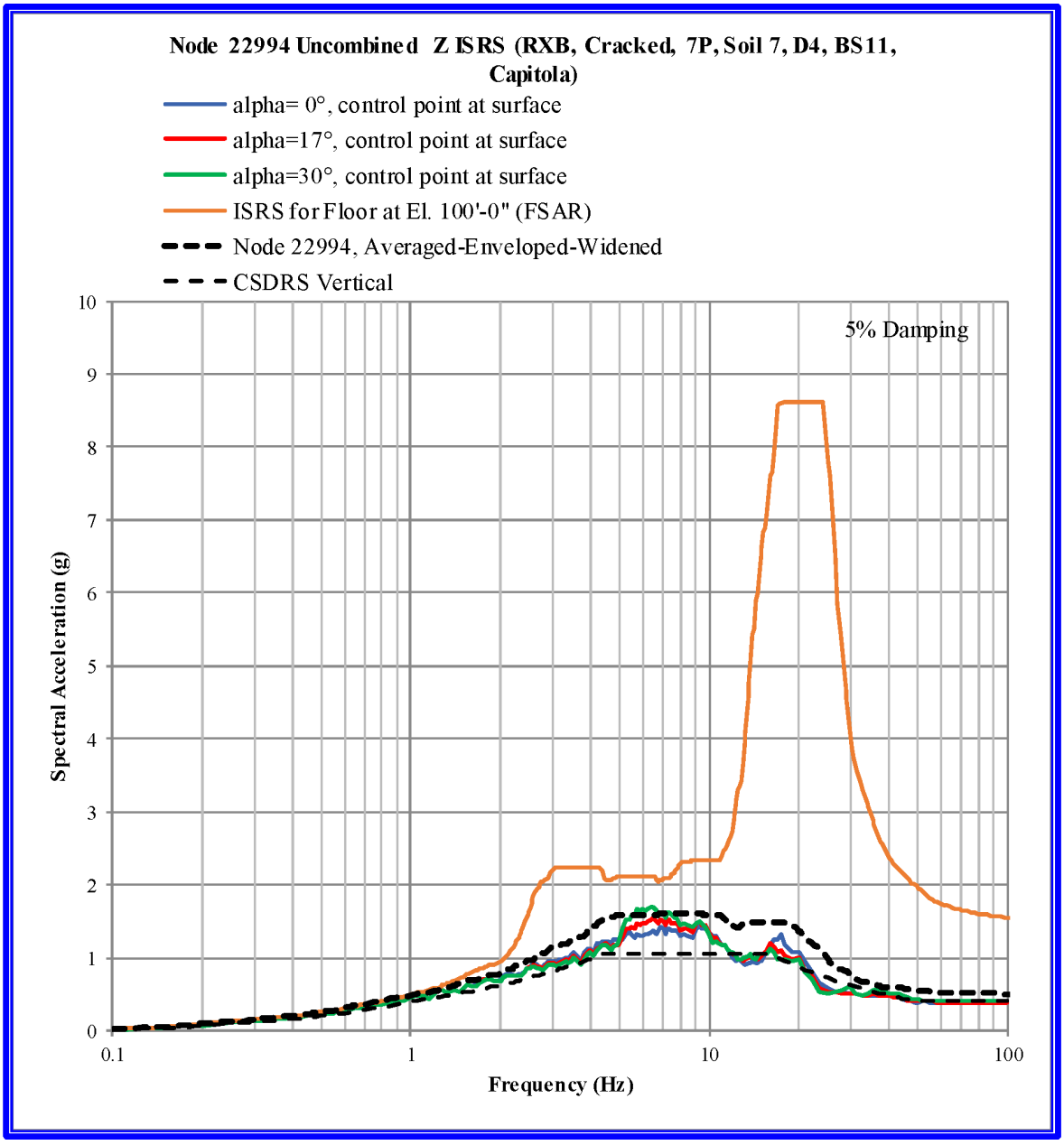

Figure 5-16. RXB - Uncombined Vertical (Z) ISRS, Node 22994, El. 100′, Spent Fuel Pool, SW Corner, Capitola Input.

5.5 Comparison of Uncombined ISRS at Node 29098 (El. 167′, Roof, SW Corner)

This section presents comparisons of the uncombined ISRS at Node 29098 (El. 167′, roof, southwest corner). Note that the α=0° curve represents the response to the CSDRS motion. The α=0°, α=17°, and α=30° curves do not include the coupling terms. Also note that the CSDRS at rock outcrop (thin dashes) is shown for reference only.

There are no floor response spectra to compare at this elevation, however, the averaged-enveloped-widened spectra at node 29098 are shown for comparison. In Figure 5-17, the α=17° curve is enveloped by the averaged-enveloped-widened ISRS. The α=30° curve is enveloped by the averaged-enveloped-widened ISRS, except for a band from 4.5 to 5.5 Hz and from 35 Hz to 100 Hz. When the average ISRS of the five time histories is used, the exceedances are expected to be smaller.

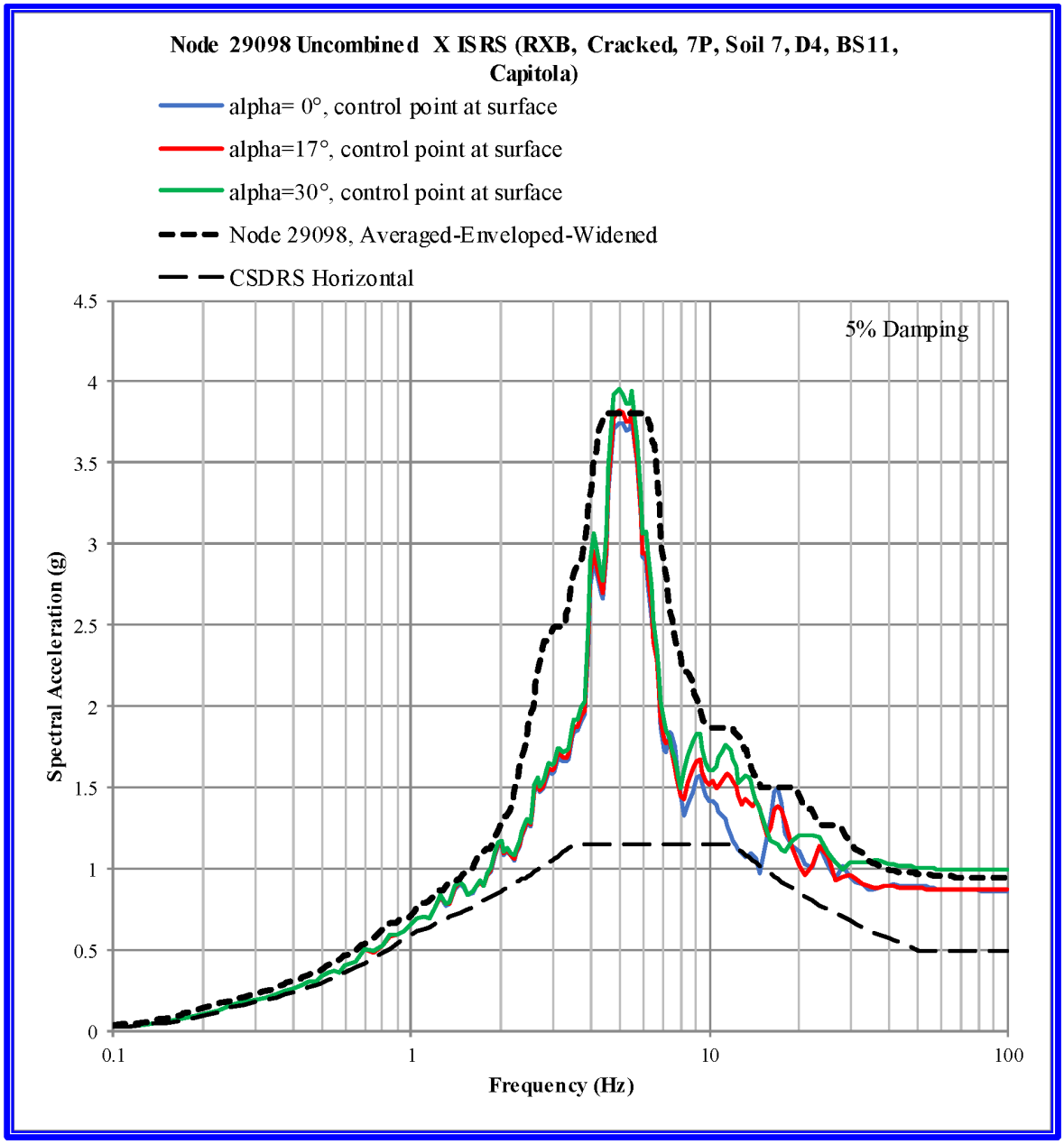

Figure 5-17. RXB - Uncombined East-West (X) ISRS, Node 29098, El. 167′, Roof, SW Corner, Capitola Input.

In Figure 5-18, the averaged-enveloped-widened ISRS curve at node 29098 envelopes the α=17° and α=30° curves except for peaks at about 5 Hz and 7 Hz. When the average ISRS of the five time histories is used, the exceedances are expected to be smaller.

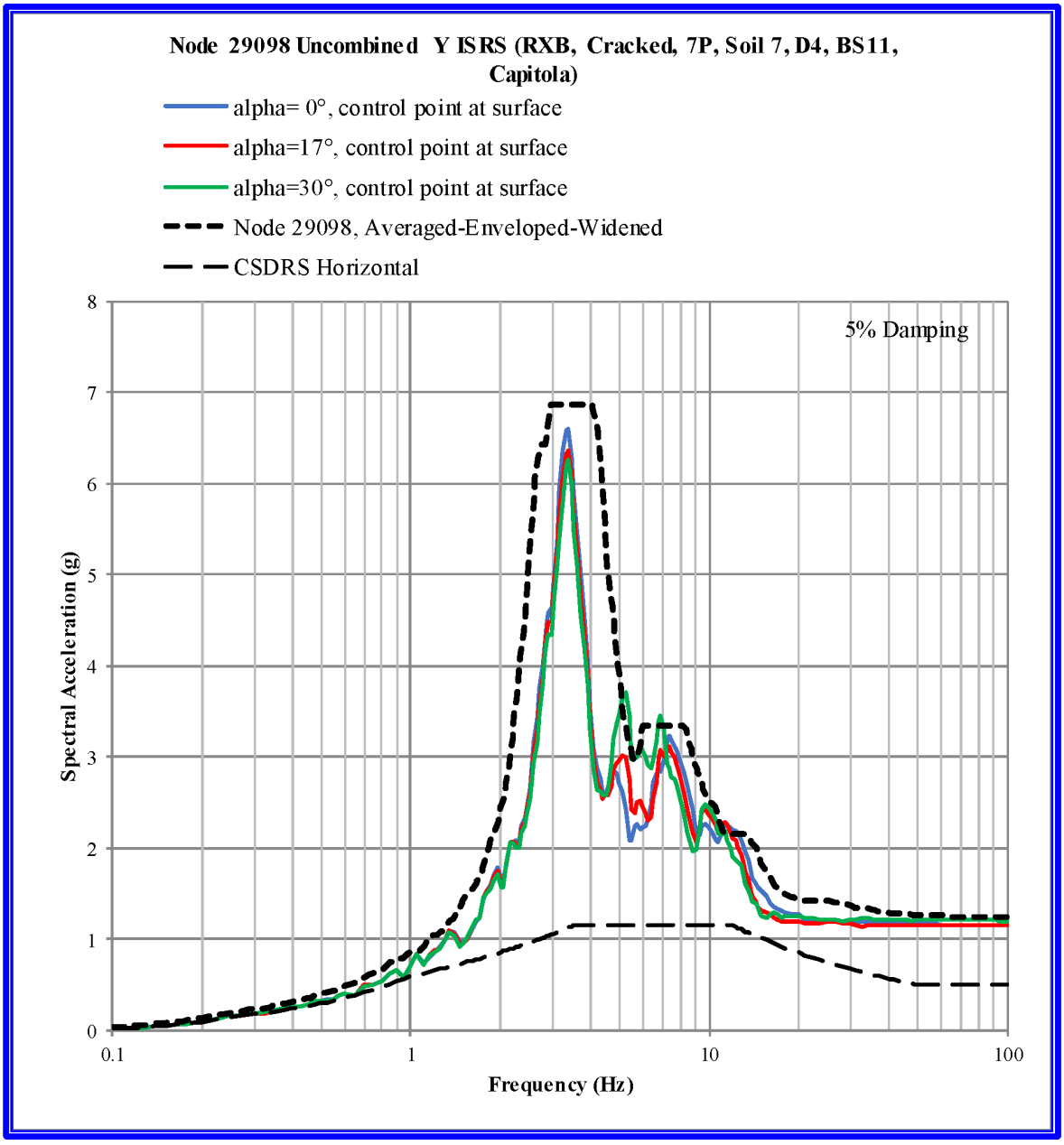

Figure 5-18. RXB - Uncombined North-South (Y) ISRS, Node 29098, El. 167′, Roof, SW Corner, Capitola Input.

In Figure 5-19, the averaged-enveloped-widened ISRS curve at node 29098 envelopes the α=17° and α=30° curves.

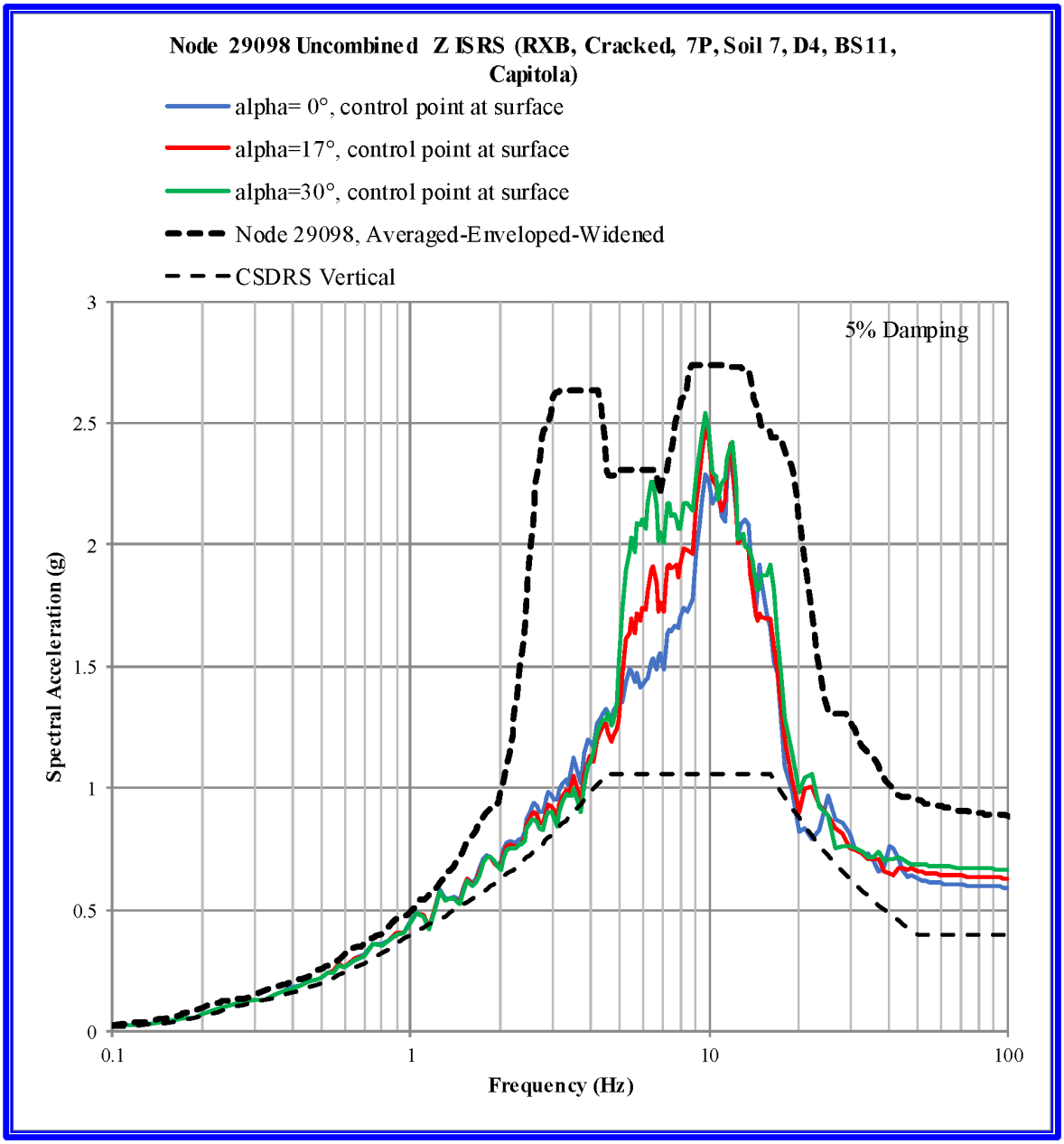

Figure 5-19. RXB - Uncombined Vertical (Z) ISRS, Node 29098, El. 167′, Roof, SW Corner, Capitola Input.

5.6 Comparison of Uncombined ISRS at Node 30350 (El. 181′, Roof Center)

This section presents comparisons of the uncombined ISRS at Node 30350 (El. 181′, roof center). Note that the α=0° curve represents the response to the CSDRS motion. The α=0°,

α=17°, and α=30° curves do not include the coupling terms. Also note that the CSDRS at rock outcrop (thin dashes) is shown for reference only.

In Figure 5-20, the floor ISRS curve envelopes the α=17° and α=30° curves.

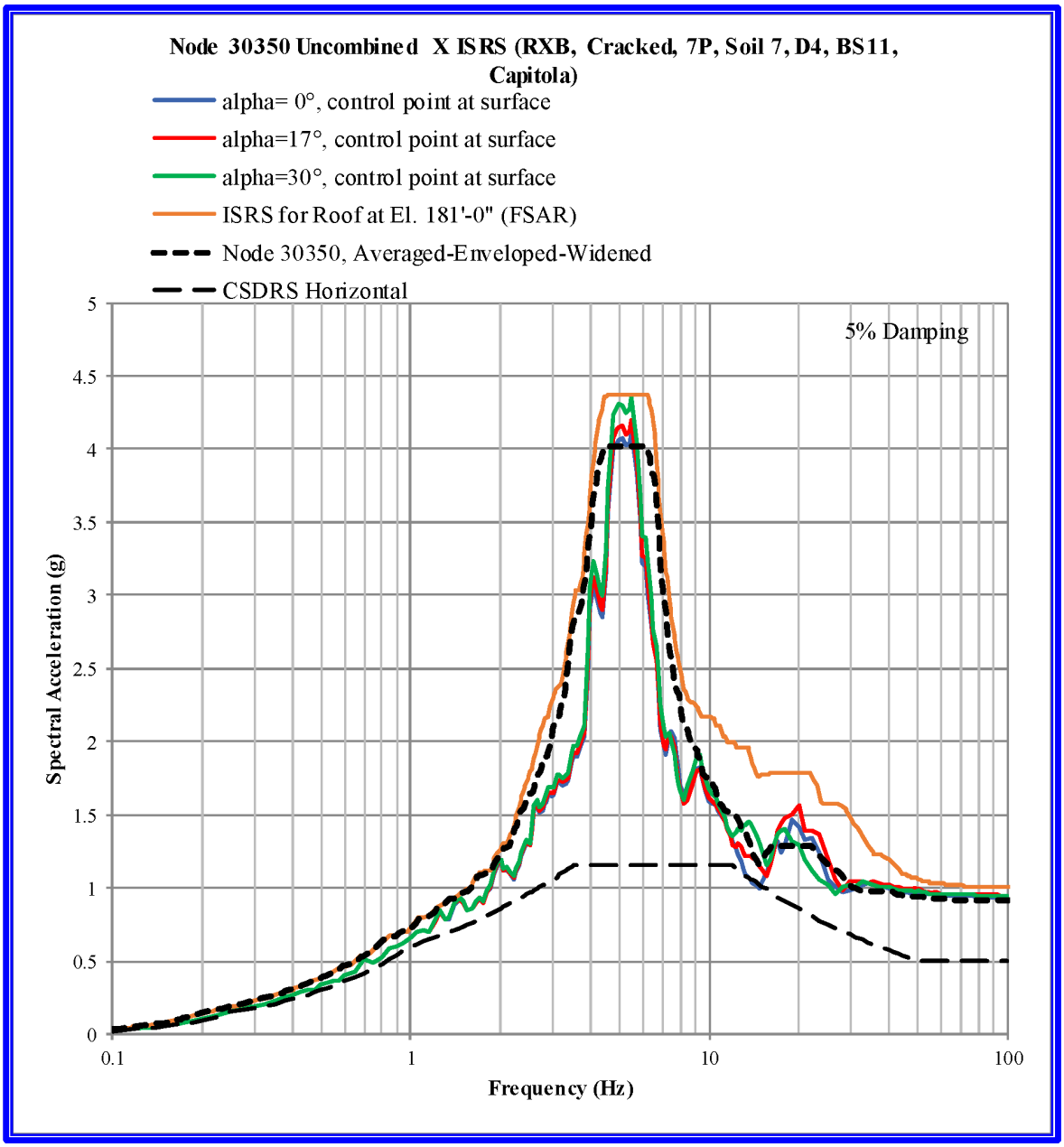

Figure 5-20. RXB - Uncombined East-West (X) ISRS, Node 30350, El. 181′, Roof Center, Capitola Input.

In Figure 5-21, the floor ISRS curve envelopes the α=17° and α=30° curves, except for peaks at 3.3 Hz, 7 Hz, 8.5 Hz, and 10 Hz. When the average ISRS of the five time histories is used, the exceedances are expected to be smaller.

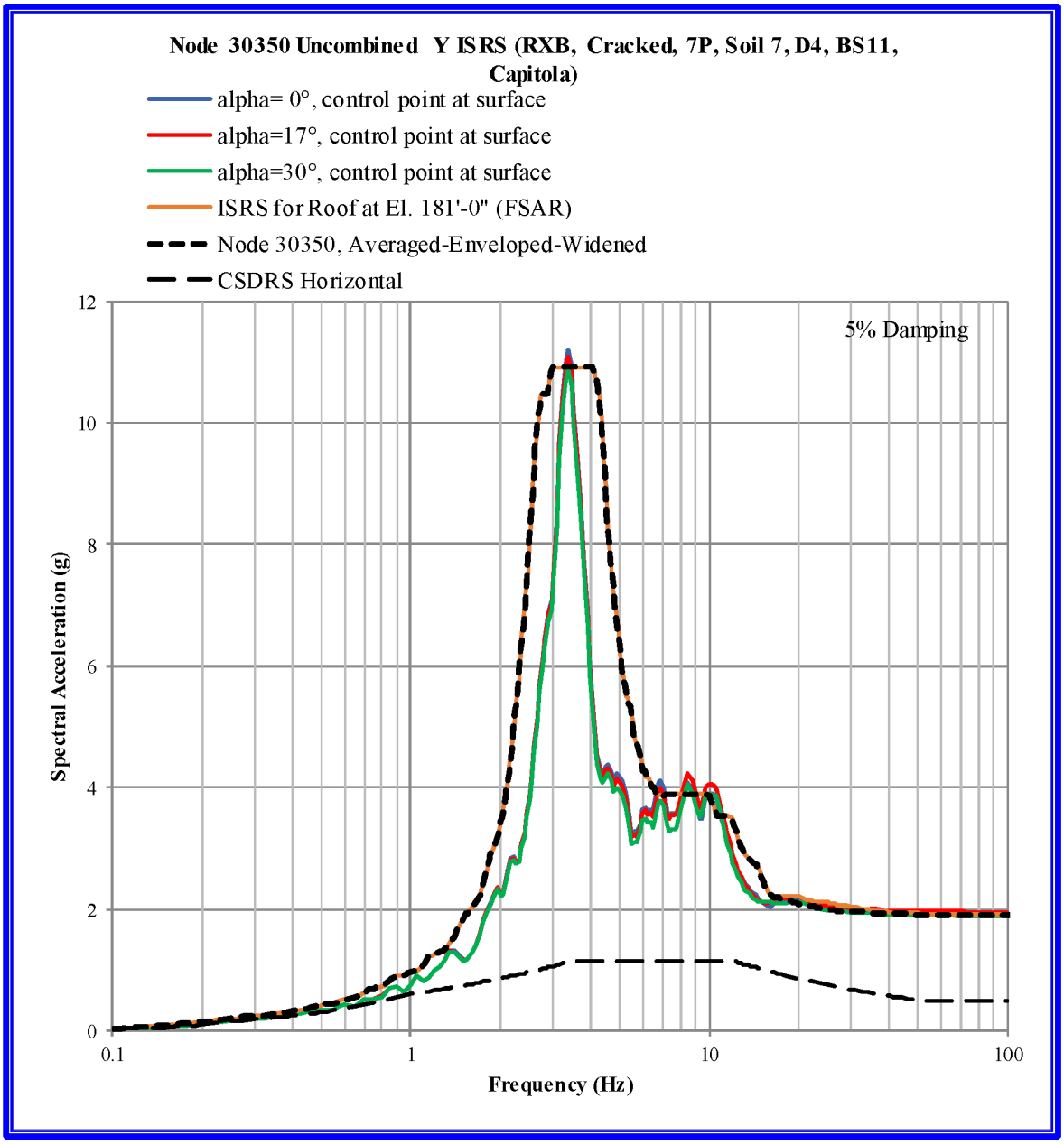

Figure 5-21. RXB - Uncombined North-South (Y) ISRS, Node 30350, El. 181′, Roof Center, Capitola Input.

In Figure 5-22, the floor ISRS curve envelopes the α=17° and α=30° curves, except for peaks at 3.5 Hz and from 30 to 100 Hz. When the average ISRS of the five time histories is used, the exceedances are expected to be smaller.

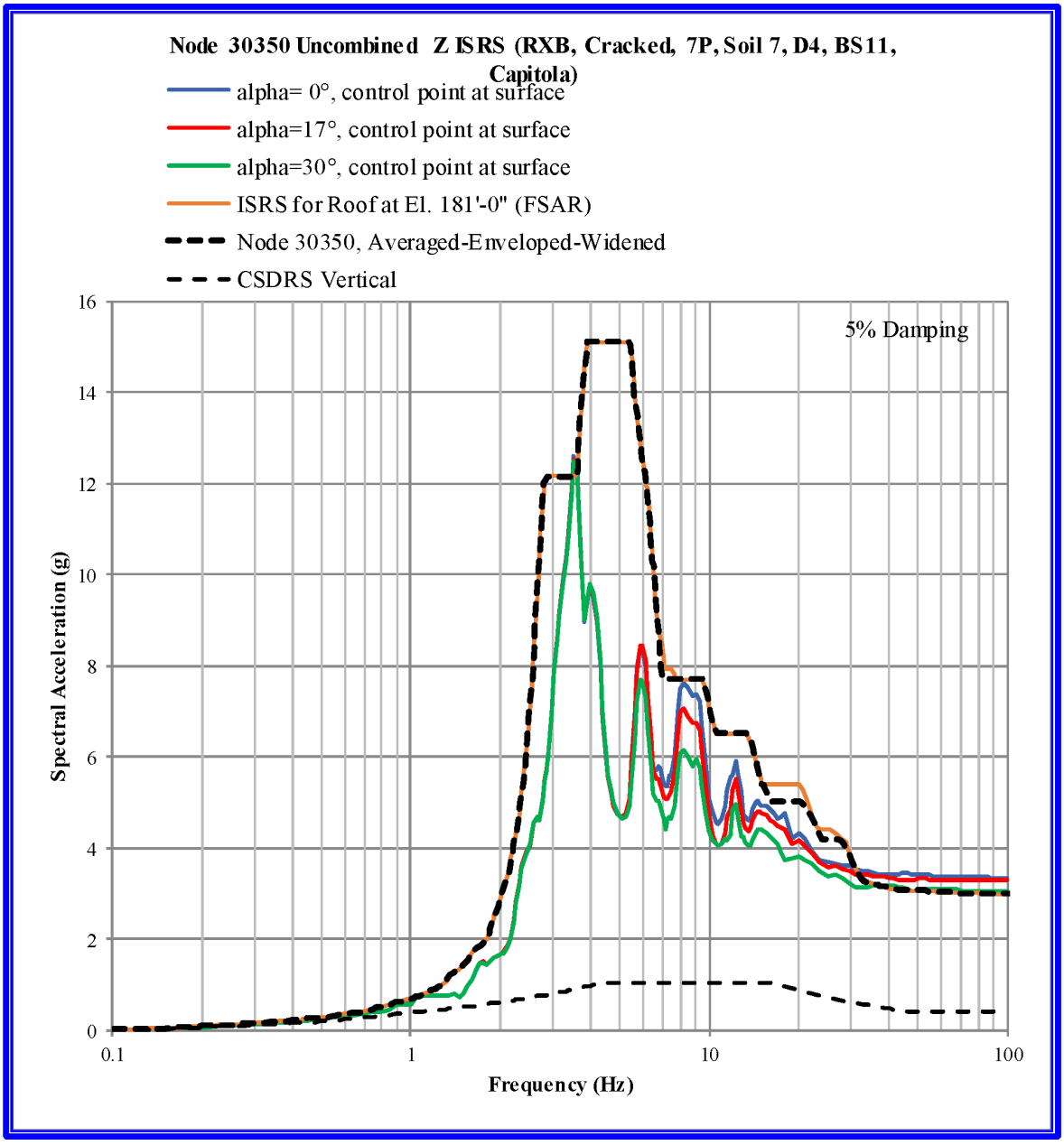

Figure 5-22. RXB - Uncombined Vertical (Z) ISRS, Node 30350, El. 181′, Roof Center, Capitola Input.

6.0 CONCLUSION

This study, first, establishes a procedure for evaluating a structure for non-vertically propagating seismic waves, and second, analyzes the RXB DCA model with non-vertically propagating seismic waves.

The intent of this SSI analysis study with non-vertically propagating (that is, inclined) waves is to compare the SSI results with those of the design-basis case, which uses conventional, vertically propagating shear (SV and SH) and P-waves for the seismic input. A body wave (either SV or P-wave) propagating at an inclined angle will include both horizontal and vertical motions in the free field and an inclined SH-wave generates only horizontal motion in the free field.

Soil Type 7 was selected for the free-field soil properties because it is nearly a uniform soil profile with a high shear wave velocity, Vs, of 5,000 ft/sec. Using a uniform and stiff soil for this study will yield conservative results, because, for non-uniform and soft soil profiles, the angle of incidence decreases as the wave propagates toward the surface, due to Snell's law and, thus, the effect of non-vertically propagating waves will be much less.

Analyses were performed and results compared for the following angles of incidence, α, where α is measured from the vertical axis:

α = 0° or apparent wave velocity = ∞, that is, the vertically propagating wave case

α = 17° or apparent wave velocity ≈ 5,000 / sin(17°) = 17,100 ft/sec (5.2 km/sec)

α = 30° or apparent wave velocity ≈ 5,000 / sin(30°) = 10,000 ft/sec (3.0 km/sec).

For the non-vertically propagating wave cases, the control point must be at the surface. If the control point were at the foundation level, there would be a shift in the soil column frequency of inclined waves. But because the in-layer motion at the foundation level is determined for α = 0°, there would be a mismatch in the soil column frequency between the in-layer motion and the non-vertically propagating wave. This would result in incorrect responses being generated.

Note that in the comparison of acceleration response spectra (ARS) in the free field (Section 3.2), the α = 0° (vertically propagating) curve represents the CSDRS case. The results presented in Section 3.2 show the effect of the coupling terms due to non-vertically propagating waves. These results show that, even though the horizontal input motion at the surface is the same for all angles of incidence of inclined SV waves (Figure 3-2), the motion at the foundation depth exceeds that of the CSDRS (or FIRS), even without including the coupling terms from inclined waves. For example, see Figure 3-8. Once coupling terms from inclined waves are considered, the motion at the foundation depth far exceeds those of the CSDRS responses. For example, see Figure 3-9. Therefore, the coupling terms from inclined waves should not be

included in the response calculation, in order to properly maintain the as-defined design-basis seismic inputs, the CSDRS and CSDRS-HF.

The SSI results of the RXB subjected to non-vertically propagating waves are provided in Section 5.0. Comparisons of ISRS results for all angles of incidence with the broadened, design ISRS show that there are only small exceedances, at a few locations, at narrow frequency bandwidths. These exceedances, as summarized in Section 3.3, are due to the fact that the free-field, in-layer motions for inclined waves at depth exceed the corresponding motions from the CSDRS with vertically propagating waves, resulting in an effective SSI input motion that is higher than the CSDRS input motion.

Finally, it is concluded that combining the coupling responses due to non-vertically propagating waves can lead to overly conservative and incorrect structural responses. When combining the horizontal responses due to inclined SV-waves with the horizontal responses due to inclined P-waves, it is implied that the corresponding coupling responses in the free field at the foundation level are also combined. This combination of the free-field responses at the foundation level due to inclined waves results in response spectra at the foundation level which are much higher than the design-basis foundation CSDRS.

SASSI2010 was used to perform the SSI analyses. Additional verification and validation of the SASSI2010 program with non-vertically propagating waves has been performed. Validation problems include the response of the free-field to inclined waves and the response of a structure to inclined waves.

Kinematic interaction and sidewall impedance are implicitly included in the SASSI solver. Gaps between the soil and structure were investigated and results presented in RAI 8932, Question 3.7.2-6.

Impact on DCA:

FSAR Tier 2, Section 3.7.2.1.1.3 and FSAR Tier 2, Figures 3.7.2-149 through 3.7.2-155 have been revised as described in the response above and as shown in the markup provided in this response.

forces due to soil separation are within design margins of the building components, leaving the building design unaltered. See Figure 3.7.2-136 through Figure 3.7.2-141 and Table 3.7.2-41 and Table 3.7.2-43.

RAI 03.07.02-6

Based on the results of these studies, it is concluded that modeling the structures as fully embedded is an acceptable design approach.

RAI 03.07.02-6S1

COL Item 3.7-11: A COL applicant that references the NuScale Power Plant design certification will perform a site-specific analysis that, if applicable, assesses the effects of soil separation. The COL applicant will confirm that the in-structure response spectra in the soil separation cases are bounded by the in-structure response spectra shown in FSAR Figure 3.7.2-107 through Figure 3.7.2-122.

RAI 03.07.02-23

Effect of Non-Vertically Propagating Seismic Waves

RAI 03.07.02-23

A sensitivity study was performed to determine the effect of non-vertically propagating shear waves. This study, first, establishes a procedure for evaluating a structure that experiences non-vertically propagating seismic waves, and second, analyzes the RXB DCA model with non-vertically propagating seismic waves.

RAI 03.07.02-23

The intent of the SSI analysis study with non-vertically propagating (that is, inclined) waves is to compare the SSI results with those of the design-basis case, which uses conventional, vertically propagating shear (SV and SH) and P-waves for the seismic input. A body wave (either SV- or P-wave) propagating at an inclined angle will include both horizontal and vertical motions in the free field, whereas an inclined SH-wave generates only horizontal motion in the free field.

RAI 03.07.02-23

For the sensitivity study, Soil Type 7 was selected for the free-field soil properties because it is a nearly uniform soil profile with a high shear wave velocity, Vs, of 5,000 ft/sec. Using a uniform and stiff soil for this study will give conservative results because, for non-uniform and soft soil profiles, the angle of incidence decreases as the wave propagates toward the surface, due to Snell's law and, thus, the effect of non-vertically propagating waves will be much less.

RAI 03.07.02-23

Analyses were performed and results compared for the following angles of incidence, α, where α is measured from the vertical axis (see Figure 3.7.2-149):

RAI 03.07.02-23

α = 0° or apparent wave velocity = ∞, that is, the vertically propagating wave case

RAI 03.07.02-23

α = 17° or apparent wave velocity ≈ 5,000 / sin(17°) = 17,100 ft/sec (5.2 km/sec)

RAI 03.07.02-23

α = 30° or apparent wave velocity ≈ 5,000 / sin(30°) = 10,000 ft/sec (3.0 km/sec).

RAI 03.07.02-23

For the non-vertically propagating wave cases, the control point must be at the surface. If the control point were at the foundation level, there would be a shift in the soil column frequency of inclined waves. But because the in-layer motion at the foundation level is determined for α = 0°, there would be a mismatch in the soil column frequency between the in-layer motion and the non-vertically propagating wave. This would result in incorrect responses being generated. Therefore, the control point is taken at the surface.

RAI 03.07.02-23

Free Field Acceleration Response Spectra

RAI 03.07.02-23

When combining the horizontal responses due to inclined SV-waves with the horizontal responses due to inclined P-waves, it is implied that the corresponding coupling responses in the free-field at the foundation level are also combined. This combination of the free-field responses at the foundation level due to inclined waves results in response spectra at the foundation level which are much higher than the design-basis, foundation CSDRS and, thus, violate the design basis of the plant.

RAI 03.07.02-23

In the comparison of acceleration response spectra (ARS) in the free field, the α = 0° (vertically propagating) curve represents the CSDRS case. The results from this case show the effect of the coupling terms due to non-vertically propagating waves. These results show that, even though the horizontal input motion at the surface is the same for all angles of incidence of inclined SV waves (Figure 3.7.2-150) the motion at the foundation depth exceeds those of the CSDRS (or FIRS) even without including the coupling terms from inclined waves. For example, see Figure 3.7.2-151. Figure 3.7.2-150 shows the X-response ARS at the surface due to SV-waves for α = 0°, 17°, and 30°. Note that these curves are identical because the control point is at the ground surface. The CSDRS at the rock outcrop (dashed line) is shown for reference only. All three ARS at the surface due to SV-waves for α = 0°, 17°, and 30° are identical. Once coupling terms from inclined waves are considered, the motion at the foundation depth far exceeds those of the CSDRS responses. For example, see Figure 3.7.2-152. Therefore, the coupling terms from inclined waves should not be included in the response calculation in order to properly maintain the as-defined design-basis seismic inputs, the CSDRS and CSDRS-HF.

RAI 03.07.02-23

Note that in the legends of the figures, "X/SV" means the X-response due to SV-wave input; "X/P" means the X-response due to P-wave input; "Y/SH" means the Y-response due to SH-wave input; etc. Also, when a response is referred to as "CSDRS," it means the "response due to the CSDRS-compatible input time history."

RAI 03.07.02-23

ISRS Results

RAI 03.07.02-23

The SSI effects due to the RXB being subjected to non-vertically propagating waves are also studied. Comparisons of ISRS results for all angles of incidence with the broadened design ISRS show that there are exceedances at a few locations at narrow frequency bandwidths. These exceedances are due to the fact that the free-field within (in-layer) motions for inclined waves at depth exceed the corresponding motions from the CSDRS with vertically propagating waves, resulting in an effective SSI input motion that is higher than the CSDRS input motion. For a sample of results, see Figure 3.7.2-153 through Figure 3.7.2-155. In addition, if the complete set of time histories were used, the ISRS would smooth out and flatten.

RAI 03.07.02-23

Finally, it is concluded that combining the coupling responses due to non-vertically propagating waves can lead to overly conservative results. The combination of the free-field responses at the foundation level due to inclined waves results in a design response spectrum which is much higher than the CSDRS.

3.7.2.1.2 Finite Element Models

RAI 03.07.02-1

Meshing of the area elements was done automatically using SAP2000 by defining a maximum element size in each direction. The aspect ratios were also kept as low as possible (closer to square shape), and internal sharp angles were avoided.

RAI 03.07.02-1

Meshing for both the RXB and CRB models were refined further, and it is shown that further refinement does not affect the structural response. The mesh refinement was done by dividing each side of the area elements into two, breaking each element to four elements. The structural responses compared include both local and global responses of the structure. The comparison shows that effects of further mesh refinement on the structural response is negligible. In addition to the modal analysis, to compare the natural frequencies and mass participation ratios, static analysis cases due to 1g loading in the x, y or z directions were used to make different comparisons. Soil elements' height were determined based on 1/5th of the wave length.

RAI 03.07.02-23

Figure 3.7.2-149: Non-Vertically Propagating Seismic Wave RXB Sensitivity Analysis Cases

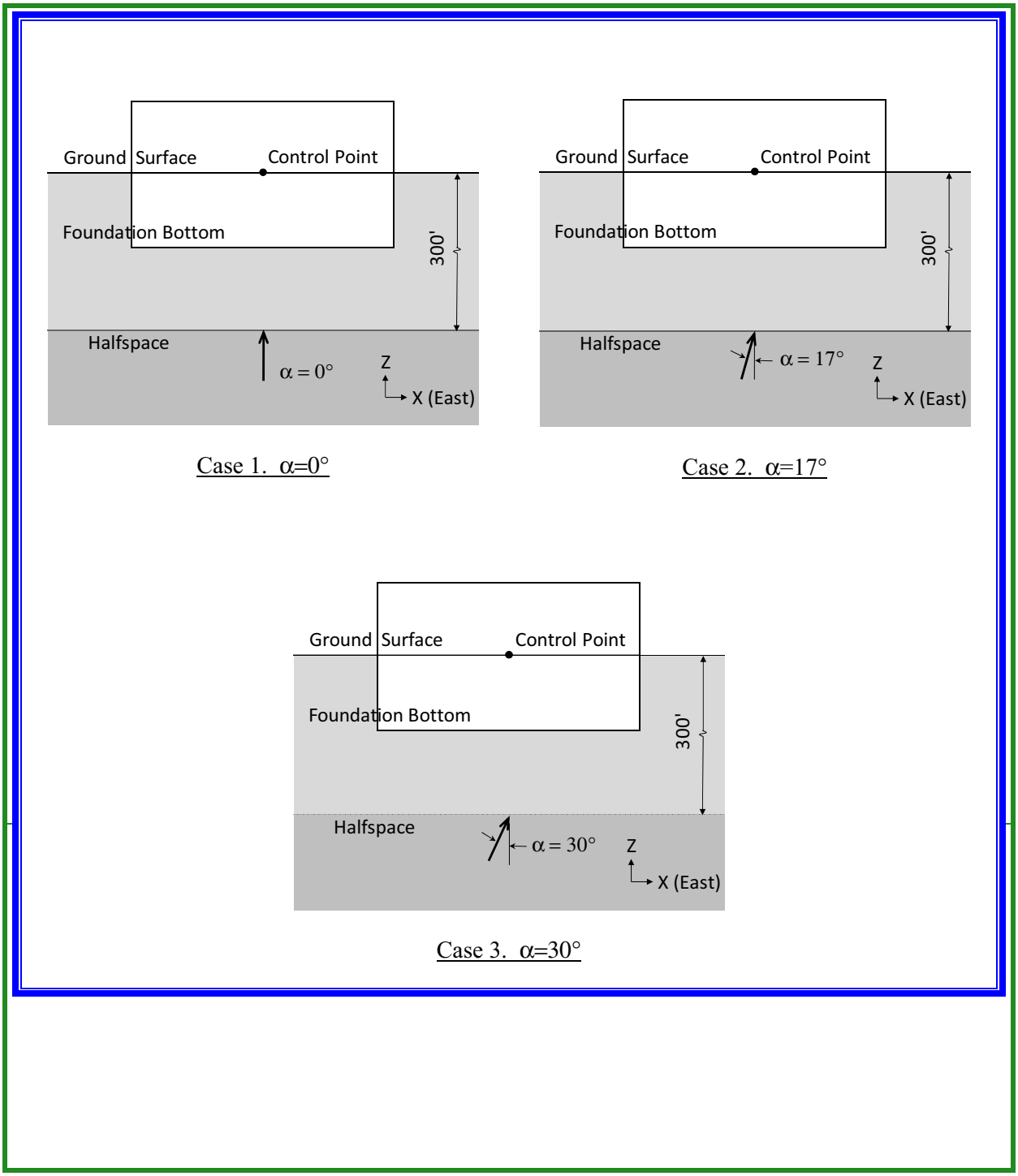

RAI 03.07.02-23

Figure 3.7.2-150: Non-Vertically Propagating Seismic Wave Sensitivity Study with Soil Type 7 - Free Field Uncoupled East-West (X) ARS at Surface, Capitola Input

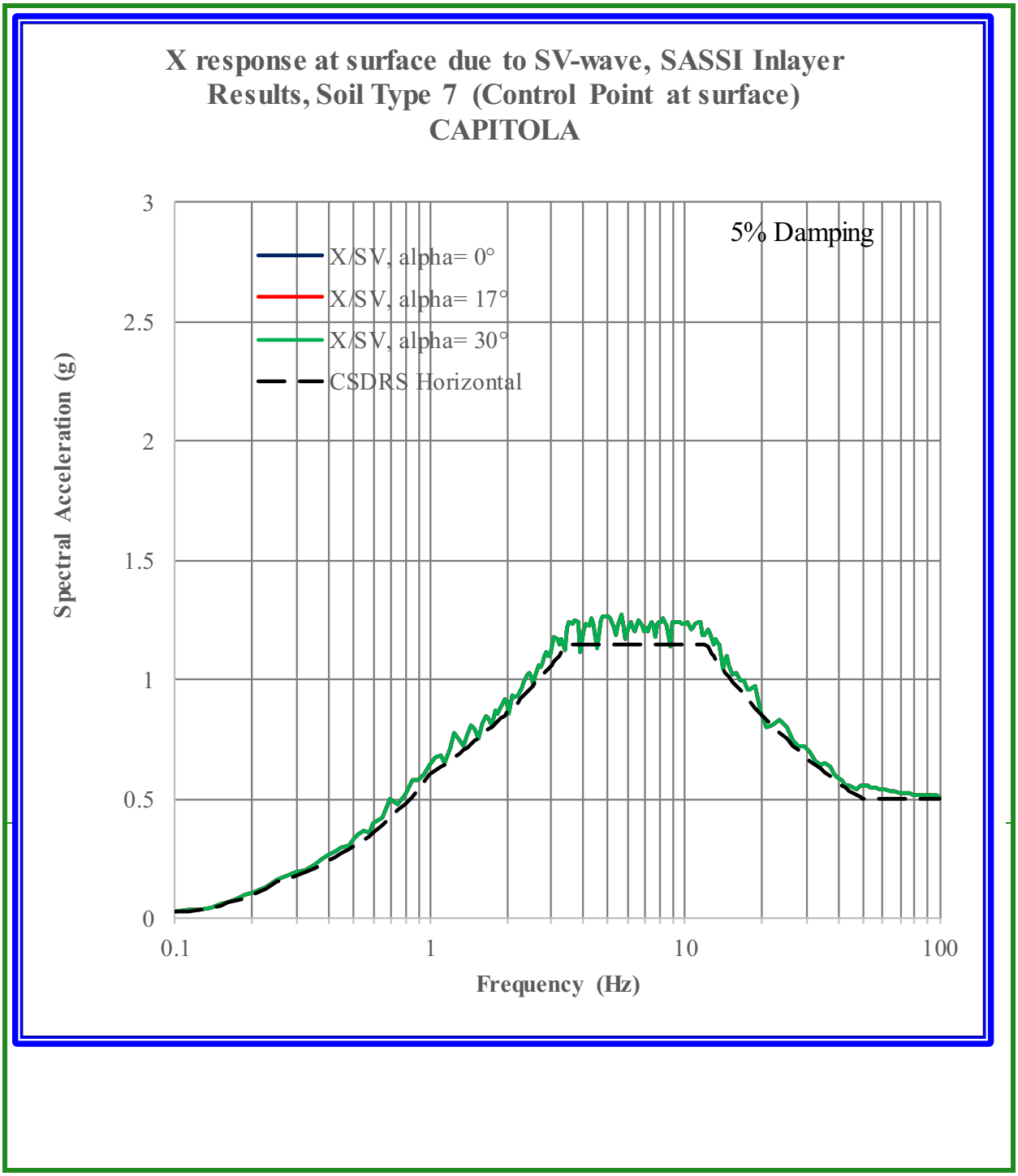

RAI 03.07.02-23

Figure 3.7.2-151: Non-Vertically Propagating Seismic Wave Sensitivity Study with Soil Type 7 - Free Field East-West (X) ARS Depth 85', Capitola Input, Alpha = 30 degrees

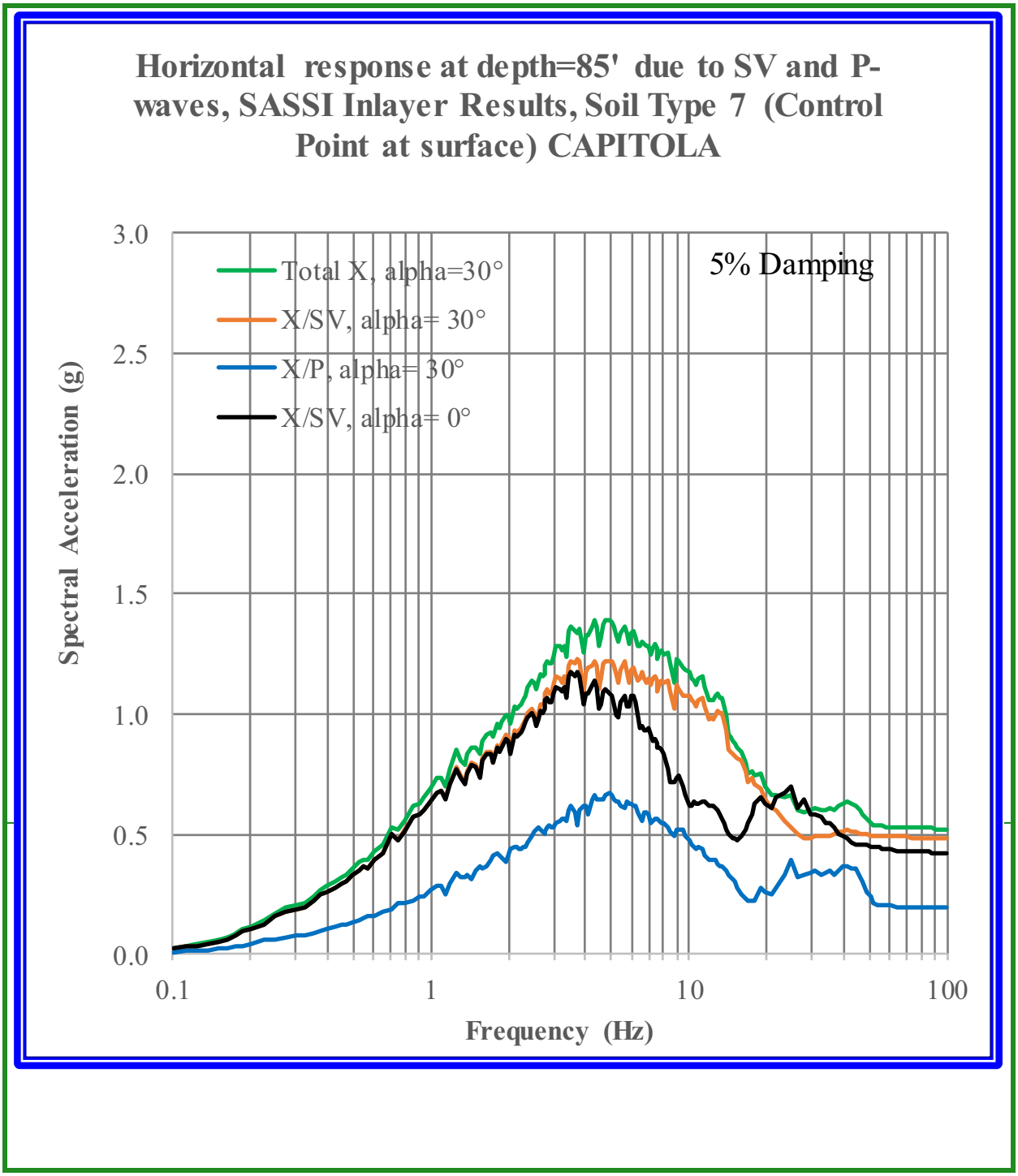

RAI 03.07.02-23

Figure 3.7.2-152: Non-Vertically Propagating Seismic Wave Sensitivity Study with Soil Type 7 - Comparison of Combined Free-Field East-West (X) ARS at Depth 85', Capitola Input, Alpha = 0 Degrees, 17 Degrees, 30 Degrees

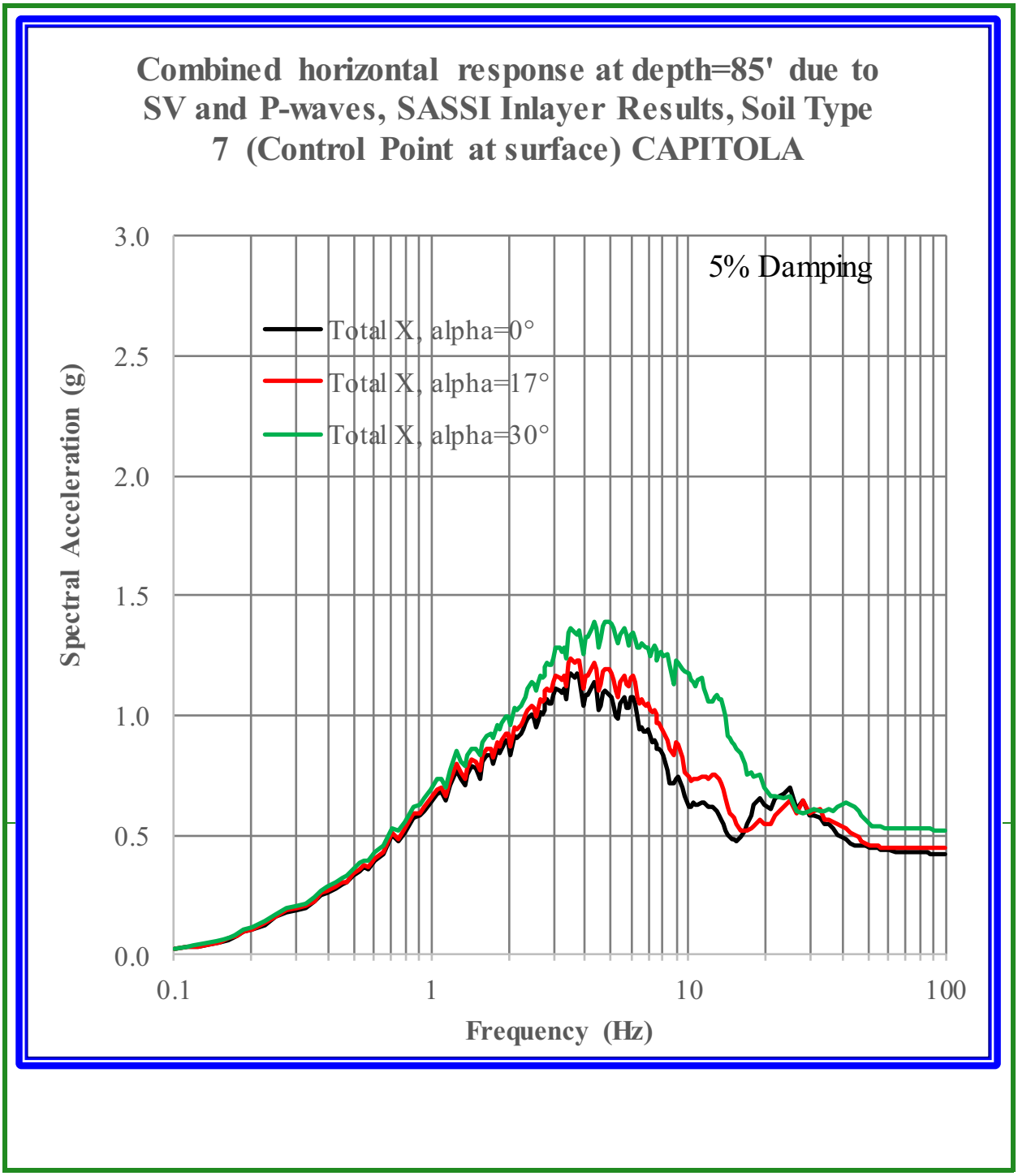

RAI 03.07.02-23

Figure 3.7.2-153: Non-Vertically Propagating Seismic Wave Sensitivity Study for the RXB - Uncombined East-West (X) ISRS, Node 3996, Top of Basemat, NW Corner, Capitola Input

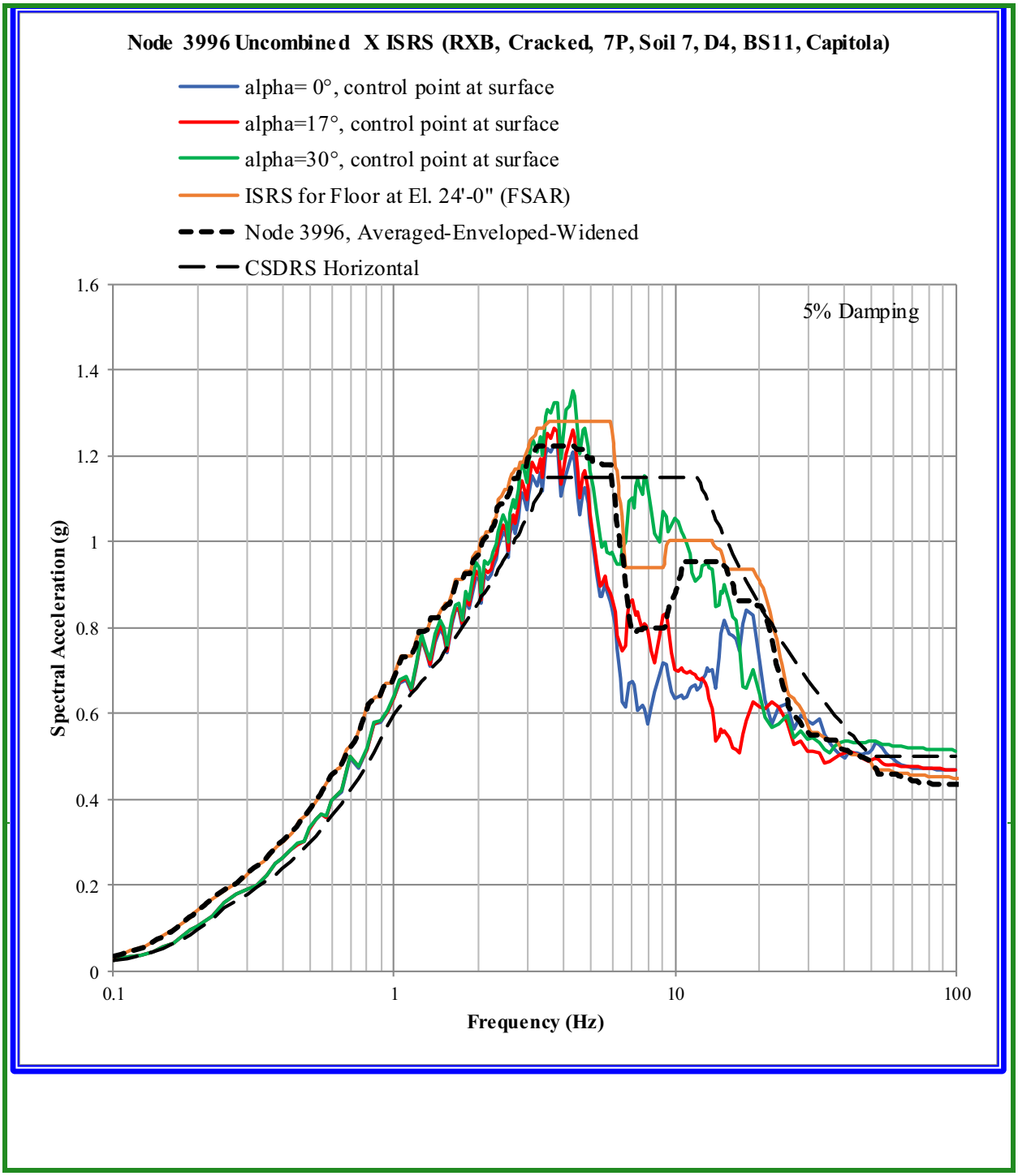

RAI 03.07.02-23

Figure 3.7.2-154: Non-Vertically Propagating Seismic Wave Sensitivity Study for the RXB – Uncombined North-South (Y) ISRS, Node 3996, Top of Basemat, NW Corner, Capitola Input

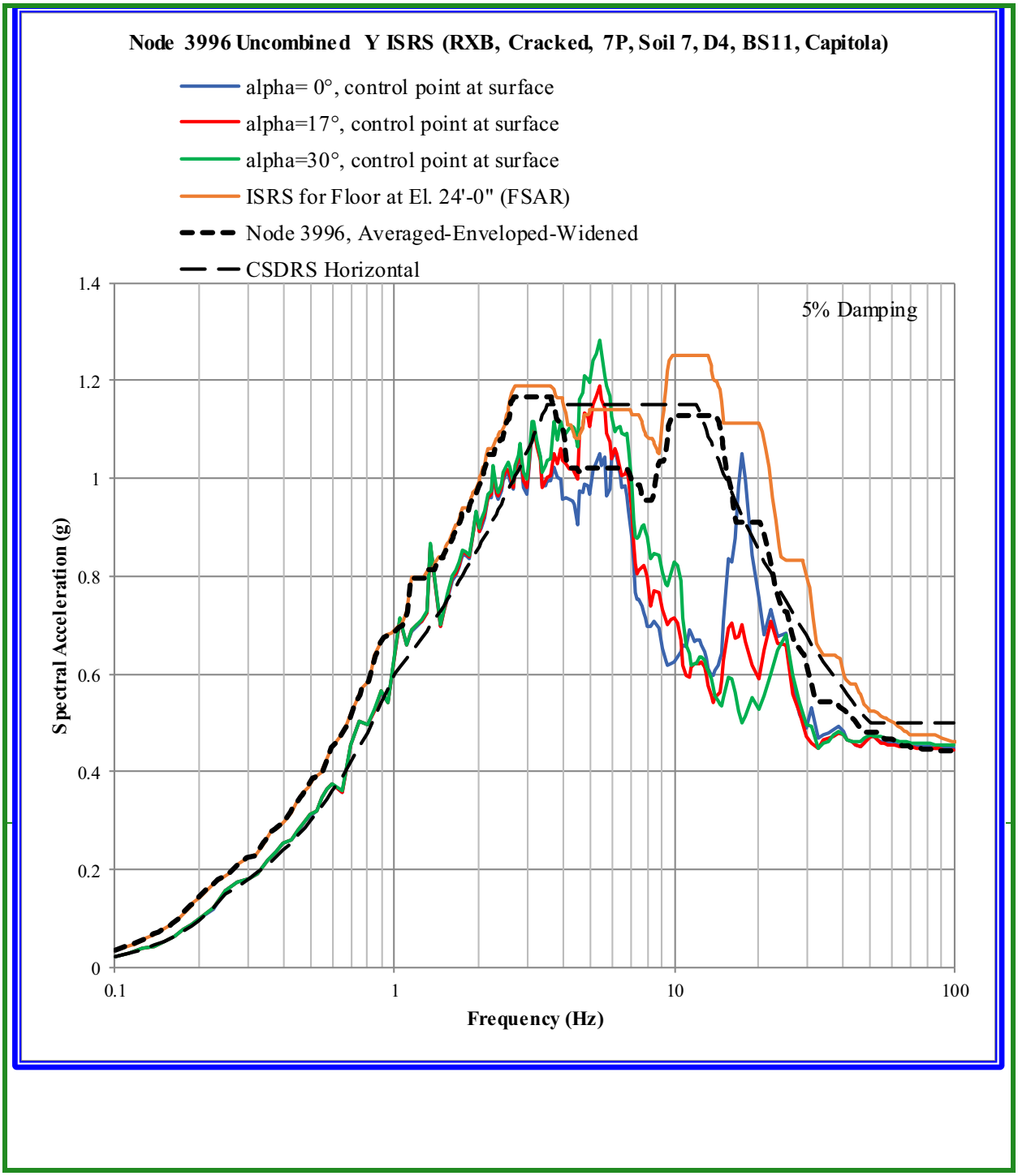

RAI 03.07.02-23

Figure 3.7.2-155: Non-Vertically Propagating Seismic Wave Sensitivity Study for the RXB – Uncombined Vertical (Z) ISRS, Node 3996, Top of Basemat, NW Corner, Capitola Input